Advances in Biological Regulation 67 (2018) 190–211

Contents lists available at ScienceDirect

Advances in Biological Regulation

journal homepage: www.elsevier.com/locate/jbior

Effects of berberine, curcumin, resveratrol alone and in combination with chemotherapeutic drugs and signal transduction inhibitors on cancer cells—Power of nutraceuticals

James A. McCubrey[a,*], Stephen L. Abrams[a], Kvin Lertpiriyapong[b,c], Lucio Cocco[d], Stefano Ratti[d], Alberto M. Martelli[d], Saverio Candido[e], Massimo Libra[e], Ramiro M. Murata[a,f], Pedro L. Rosalen[g], Paolo Lombardi[h], Giuseppe Montalto[i,j], Melchiorre Cervello[j], Agnieszka Gizak[k], Dariusz Rakus[k], Linda S. Steelman[a]

[a] Department of Microbiology and Immunology, Brody School of Medicine at East Carolina University, Greenville, NC 27858, USA
[b] Department of Comparative Medicine, Brody School of Medicine at East Carolina University, USA
[c] Center of Comparative Medicine and Pathology, Memorial Sloan-Kettering Cancer Center, Weill Cornell Medicine and the Hospital for Special Surgery, New York City, New York, USA
[d] Dipartimento di Scienze Biomediche e Neuromotorie, Università di Bologna, Bologna, Italy
[e] Department of Biomedical and Biotechnological Sciences – Oncological, Clinical and General Pathology Section, University of Catania, Catania, Italy
[f] Department of Foundational Sciences, School of Dental Medicine, East Carolina University, USA
[g] Department of Physiological Sciences, Piracicaba Dental School, State University of Campinas, Piracicaba, Brazil
[h] Naxospharma, Via Giuseppe Di Vittorio 70, Novate Milanese 20026, Italy
[i] Biomedical Department of Internal Medicine and Specialties, University of Palermo, Palermo, Italy
[j] Consiglio Nazionale Delle Ricerche, Istituto di Biomedicina e Immunologia Molecolare "Alberto Monroy", Palermo, Italy
[k] Department of Molecular Physiology and Neurobiology, Wroclaw University, Wroclaw, Poland

ARTICLE INFO

Keywords:
Berberine
Curcumin
Resveratrol
Metformin

ABSTRACT

Over the past fifty years, society has become aware of the importance of a healthy diet in terms of human fitness and longevity. More recently, the concept of the beneficial effects of certain components of our diet and other compounds, that are consumed often by different cultures in various parts of the world, has become apparent. These "healthy" components of our diet are often referred to as nutraceuticals and they can prevent/suppress: aging, bacterial, fungal and viral infections, diabetes, inflammation, metabolic disorders and cardiovascular diseases and have other health-enhancing effects. Moreover, they are now often being investigated because of their anti-cancer properties/potentials. Understanding the effects of various natural products on cancer cells may enhance their usage as anti-proliferative agents which may be beneficial for many health problems. In this manuscript, we discuss and demonstrate how certain nutraceuticals may enhance other anti-cancer drugs to suppress proliferation of cancer cells.

1. Introduction

Berberine (BBR), curcumin (CUR) and resveratrol (RES) are examples of three commonly consumed nutraceuticals which have been investigated for prevention/treatment of various diseases and ailments for centuries (McCubrey et al., 2017a, 2017b). These and

* Corresponding author.
E-mail address: mccubreyj@ecu.edu (J.A. McCubrey).

http://dx.doi.org/10.1016/j.jbior.2017.09.012
Received 25 September 2017; Accepted 29 September 2017
Available online 03 October 2017

other nutraceuticals are contained in different components of our diet, such as; fruits, berries, grapes, spices obtained from plants such as turmeric, oils from plants and fish and in addition leaves from various plants and trees. In general, they are not toxic at doses that we consume normally. Moreover, they have been associated with long life and the prevention of common health problems such as: cardiovascular, bacterial, fungal and viral infections, diabetes, inflammation and even obesity. There are many other nutraceuticals. Other commonly consumed nutraceuticals are olive oil and fish oil. More recently they have been investigated for their anti-cancer and anti-aging effects, two processes which are often intimately related (Cusimano et al., 2017).

Nutraceuticals can affect neurological processes. It turns out that signaling pathways are dysregulated in neurological diseases such as: Alzheimer's disease (AD), Amyotrophic lateral sclerosis (ALS) and others (Tomita, 2017; Bradshaw et al., 2015; Shamseddine et al., 2015; Tu-Sekine et al., 2015; Aditi et al., 2016; Rohacs, 2016; Giudici et al., 2016; Yang et al., 2016; Kang et al., 2016; Hayashi et al., 2016 Scarlata et al., 2016; Ghim et al., 2016; Raben and Barber, 2017). The PI3K/PTEN/Akt/mTORC1/GSK-3 signaling pathway is often regulated by nutraceuticals and it plays critical roles in: diabetes, cardiovascular diseases, inflammation, neurology, obesity, as well as cancer (Lupieri et al., 2015; Guidetti et al., 2015; Beretta et al., 2015; Mikoshiba, 2015; Huang and Natarajan, 2015; McCubrey et al., 2017c, 2017d,; Carman and Han, 2017; Hermida et al., 2017; Gowda et al., 2017a,b; Nishida et al., 2017; Ricciardi et al., 2017; Ruvolo, 2017; Ruzzene et al., 2017; Hatch et al., 2017; Yamauchi et al., 2017; Shears et al., 2017; Ramazzotti et al., 2017; Schrock et al., 2017; McCubrey et al., 2017c; Coant et al., 2017; Ebenezer et al., 2017; Mérida et al., 2017; Gowda et al., 2017a,b; Campa and Hirsch, 2017; Ryuno et al., 2017). One of the first and most effective drugs to treat certain neurological diseases is lithium which is often administered to manic depressive patients. A target of lithium is GSK-3 which is a key component of the PI3K/PTEN/AKT/mTORC1/GSK-3, WNT-beta-catenin pathways and others (McCubrey et al., 2017a, 2017b).

BBRs are contained in many plants and fruits including: *Berberis aetnensis C. Presl.*, *Berberis aristata*, *Berberis vulgaris*, *Coptis chinensis*, *Coptis japonica*, *Coptis rhizome*, *Hydrastis canadensis*, *Phellondendron amurense* and *Tinosora cordifolia*. BBR is an isoquinoline quaternary alkaloid (a 5,6-dihydrodibenzo [a,g]quinolizinium derivative). The health promoting effects of BBR has been known for centuries. BBR is often used in traditional Chinese and Indian medicine and is frequently consumed.

BBR, like CUR and RES, are sometimes considered dietary supplement. However, certain fruits containing BBR can be purchased over the counter at many different types of stores. BBR is also consumed for alleviation of various conditions/diseases such as: abdominal pain, coronary artery disease, diabetes, diarrhea, fatty liver disease, gastroenteritis, hyperlipidemia, hypertension, metabolic syndrome, neurodegeneration, obesity, polycystic ovary syndrome (McCubrey et al., 2017a, 2017b, 2017c; McCubrey and Cocco, 2017) BBR is being examined in at least 35 clinical trials.

A new aspect of BBR may be in the treatment of certain cancers. BBR is believed to have anti-diabetic, anti-inflammatory and anti-microbial (both anti-bacterial and anti-fungal) properties. BBRs can influence the expression of various genes that are involved in: apoptosis, autophagy, metastasis and proliferation such as: BCL2, BCLXL, PARP1, Beclin-1, TP53, $p21^{Cip1}$, MMP9 (Cordell et al., 2001; Tillhon et al., 2012). In addition, BBRs may induce double strand DNA breaks and cell cycle arrest (Wang et al., 2012). These properties of BBR may be related to its potential anti-cancer effects.

BBRs may interact with DNA and RNA via the nitrogen atom at the 7-positon in the alkaloid BBR skeleton. This interaction between BBR and nucleic acids may inhibit telomerases and topoisomerases (Qin et al., 2007; Kim et al., 1998; Gatto et al., 1996; Bhowmik et al., 2012). In addition, BBRs may influence gene transcription by interacting with the TATA-binding protein and the TATA-box present in certain promoter regions (*e.g.*, BCL2) (Xiao et al., 2012; Wang et al., 2011).

Some of the potential anti-diabetic and anti-cancer effects of BBRs are their ability to localize to the mitochondria and inhibit the electron transport chain and activate 5′ AMP-activated protein kinase (AMPK) and suppress mTOR activity (Wang et al., 2010a; Liu et al., 2011). The PI3K/PTEN/Akt/mTORC1 and Raf/MEK/ERK pathways are inhibited when AMPK is activated.

BBR can also inhibit senescence by altering gero-conversion from the process of cell cycle arrest to the induction of senescence by targeting mTOR/S6 and the generation of ROS (Zhao et al., 2013; Halicka et al., 2012).

The nutraceutical CUR is frequently obtained as an extract from the plant *Curcuma longa* (Turmeric). However, there are other compounds present in the extract which are referred to as curcuminoids. The turmeric extract consists of 60–70% CUR, 20–27% demethooxycurcumin and 10–15% bisdemethoxycurcumin (Nelson et al., 2017). These curcuminoid comprise 1–6% of the total weight of the turmeric tuber.

CUR is believed to have many health promoting properties including: anti-aging, anti-cancer, anti-hypertensive, anti-inflammatory and anti-neurological activities. The market for CUR is thought to be close to $100 million by 2022 (http://www.grandviewresearch.com/industry-analysis/turmeric-extract-curcumin-market). The effects of CUR are being examined in at least 129 clinical trials for various diseases.

CUR may exert some of its effects by altering drug transporter activity in cancer cells. CUR could enhance the anti-tumor properties of the DNA cross linking agent mitomycin C by inhibiting the expression of ATP-binding cassette transporter G2 (ABCG2, a.k.a breast cancer resistance protein, BCRP) expression. CUR treatment also increased the sensitivity of MCF-7 and MDA-MB-231 breast cancer cells to multiple chemotherapeutic drugs including: cisplatin, doxorubicin and paclitaxel and inhibited the sphere forming capacity of the cells when both CUR and a chemotherapeutic drug were added together. These events were shown to be dependent upon the suppression of ABCG2 by CUR treatment (Zhou et al., 2015a).

CUR has been shown to have effects on microRNA (miR) expression. CUR treatment of cutaneous T-cell lymphoma (CTCL) inhibited JAK-3 activity and induced miR-22 expression and suppressed the expression of many genes including: cyclin dependent kinase 2 (CDK2), histone deacetylase 6 (HDAC6), MYC associated factor X (MAX), MYC binding protein (MYCBP), nuclear receptor coactivator 1 (NCOA1), and PTEN. (Sibbesen et al., 2015).

An additional miR that is regulated by CUR is miR-34. CUR and miR-34 will regulate the expression of histone modifying enzymes. Histone modifying enzymes can affect the accessibility of promoter regions to transcription factors (Tao et al., 2013).

CUR can also suppress the PI3K/PTEN/AKT/mTORC1 pathway. CUR can induce the expression of miR-192-5b expression in A549 lung cancer cells. This resulted in decreased PI3K/PTEN/Akt/mTORC1 activity and increased apoptosis (Ye et al., 2015; Jin et al., 2015).

RES is often present in the skins of red grapes. RES is also contained in *Polygonum cuspidatum*, which is considered an invasive weed as it is related to bamboo. Historically, RES has been associated more with red wine, however, RES is also consumed as a non-alcoholic dietary supplement as a pill. It was estimated in 2012 that the global market for RES was $50 million (http://www.nutraingredients.com/Markets-and-Trends/US-dominates-global-resveratrol-market). This may be an actual underestimate today as RES is often sold in pill or liquid forms as a dietary supplement (non-alcohol based).

RES has many different effects. Perhaps one of the most studied effects of RES is the activation of sirtuins. Sirtuins are a family of proteins involved in regulation of gene expression. Many sirtuins function as histone deacetylates. The induction of sirtuins by RES has been postulated to be responsible for the beneficial effects of the Mediterranean diet (Russo et al., 2014). RES can also modulate NF-kappaB activity and inhibit cytochrome P450 isoenzyme (CYP A1) drug metabolism and cyclooxygenase activity. In addition, RES may influence TP53, FAS/FAS-ligand (FAS-L = CD95, tumor necrosis factor receptor superfamily member 6 [TNFRSF6]) induced apoptosis and mammalian target of rapamycin/mechanistic target of rapamycin (mTOR) activity. RES may also have effects on immune-regulatory cells by inducing the apoptosis of activated T cells and suppress tumor necrosis factor-alpha (TNF-alpha), interleukin 17 (IL-17) and additional pro-inflammatory cytokines (Diaz-Gerevini et al., 2016; Han et al., 2015a).

At least 110 clinical trials are or have been performed with RES. These trials examine the effects of RES on many different diseases ranging from aging, cardiovascular disorders, cancer, neurodegenerative, obesity and others. RES can activate AMPK. This important kinase is involved in insulin signaling and glucose uptake. Although it was initially studied in metabolism and metabolic diseases such as diabetes, it is now known to play essential roles in cancer as metabolism is very important in cancer development. Treatment of Neuro-2a (N2A) muscle cells with RES led to AMPK, AKT and GSK-3beta phosphorylation. The AMPK inhibitor compound C inhibited RES-mediated AMPK activation as well as AKT and GSK-3beta phosphorylation, glucose uptake and insulin signaling (Patel et al., 2011). Part of the anti-diabetic effects of the drug metformin are the induction of AMPK.

RES can have neuroprotective effects (Varamini et al., 2014; Lin et al., 2014 Abdel-Aleem et al., 2016). Often these effects are mediated at least in part by the PI3K/PTEN/AKT/mTORC/GSK-3 pathway. Treatment with RES can protect against cerebral ischemia. This was shown to be due to its anti-oxidant and oxygen free radicals scavenging abilities (Simão et al., 2012).

RES can also stimulate AMPK protein levels and ERK1,2 and AKT activation in myoblast cells. This can affect differentiation and muscle hypertrophy. Thus, REV has been postulated to be potentially useful in treatment of chronic functional and morphological muscle impairment (Montesano et al., 2013). AKT can mediate some of its effects on skeletal myotubes hypertrophy by suppressing GSK-3 (Rommel et al., 2001). GSK-3 is a key component of the PI3K/PTEN/AKT/mTORC1 and WNT/beta-catenin pathways.

RES treatment can reduce cardiac mitochondrial swelling and infarct size at reperfusion and lead to cardio-protection. Phosphorylation of GSK-3beta, which often results in its inactivation, is enhanced upon RES treatment. The mitochondrial permeability transition pore (mPTP) may be target by RES. This may lead to the translocation of GSK-3 from cytosol to mitochondrial. This permits GSK-3beta to interact with cyclophilin D to regulate mPTP (Xi et al., 2009).

GSK-3 inhibition has been shown to stimulate the interactions between muscle fructose-1,6-bisphosphatase (FBP2) and cardiac mitochondria. This protects mitochondria against swelling. In addition, the interaction of proteins involved in formation of mPTP is suppressed. This could be part of the mechanism responsible for RES-induced suppression of cardiac mitochondria swelling (Gizak et al., 2012).

Treatment of human umbilical vein endothelial cells (HUVEC) with five micromolar activates the Raf/MEK/ERK and PI3K/PTEN/AKT/mTORC1 pathways. This results in RES-mediated phosphorylation of GSK-3beta. The expression of VEGF and angiogenesis were induced at this RES concentration. However, RES at concentrations such as twenty micromolar, negative effects were observed. At the lower RES concentrations, the increase in VEGF expression was on the accumulation of beta-catenin in the nucleus possibly due to inhibition of GSK-3 activity (Wang et al., 2010b).

2. Signaling pathways affected by nutraceuticals—Common link with cancer

Nutraceuticals often exert their effects through signaling pathways such as Ras/Raf/MEK/ERK, PI3K/PTEN/AKT/mTORC1/GSK-3, JNK, JAK/STAT and TP53. These pathways are central in many biological processes (Cervello et al., 2017; McCubrey et al., 2017a, 2017b). These pathways play essential roles proliferation as well as diabetes, inflammation, and neurological disorders such as Parkinson's Disease and AD and are often aberrantly regulated in cancer. The roles of these pathways in various disorders and cancer have been recently reviewed (McCubrey et al., 2014a; McCubrey et al., 2014b; McCubrey et al., 2014c; Chappell et al., 2016; McCubrey et al., 2015; McCubrey et al., 2016; McCubrey et al., 2017c; Cariello et al., 2017; Pappas et al., 2017; Jhanwar-Uniyal et al., 2017).

Attempts to inhibit the PI3K/PTEN/Akt/mTORC1/GSK-3 and other signaling pathways have been a central focus in many pharmaceutical companies as well as basic science laboratories for the past 25 years (Kriplani et al., 2015; Fitzgerald et al., 2015; Baer et al., 2015; Jhanwar, 2015; Mollinedo and Gajate, 2015; Shears, 2015; McCubrey et al., 2015; Dusaban and Brown, 2015; Olayanju et al., 2015; Spinelli et al., 2015; Jhanwar-Uniyal et al., 2015; Carroll et al., 2015; Schurmans et al., 2015 Jahan and Davie, 2015; Barker et al., 2015 Scoumanne et al., 2016; Geck and Toker, 2016; Fields et al., 2016; Anderson et al., 2016; Maczis et al., 2016; Falasca and Ferro, 2016; Cocco et al., 2016; Tanaka et al., 2016; Perdios et al., 2016; Erneux et al., 2016; Banfic et al., 2016; Pyne et al., 2016; McCubrey et al., 2017a, 2017b).

3,5,4′-trimethoxystilbene (MR-3) is a methoxylated-derivative of RES. It has effects on MCF-7 breast and many other cancer cells.

Treatment of breast cancer cells with MR-3 resulted in increased E-cadherin expression. In contrast, treatment with MR-3 resulted in decreased SLUG, SNAIL and vimentin expression which led to decreased invasion and migration. Decreased expression and nuclear translocation of beta-catenin was observed which lead to decreased transcription of beta-catenin target genes. MR-3 treatment also suppressed AKT activity which resulted in GSK-3beta activity and suppressed AKT phosphorylation in MR-3-treated MCF-7 cells (Tsai et al., 2013). Thus, some of the targets of the RES derivative MR-3 are stimulation of GSK-3 activity.

RES can hinder the development of N-nitrosobis (2-oxopropyl)amine-induced pancreatic cancers in hamsters. RES treatment decreased both the activities of both PI3K/PTEN/AKT/mTORC1/GSK-3beta and RAF/MEK/ERK signaling pathways (Kato et al., 2015).

ROS-induced oxidative stress can have deleterious effects on mitochondrial function. RES can protect mitochondria against ROS-induced stress by inhibition of GSK-3beta. RES can regulate the activities of AMPK, liver kinase B1 (LKB1) and sirtuin 1 (SIRT1). In HEPG2 liver cells, treatment with RES resulted in suppression of apoptosis, glutathione depletion and ROS production. These events are normally mediated by arachidonic acid (AA) and iron. siRNA knock-down of LKB1 lead to AMPK inhibition. Suppression of AMPK decreased the ability of RES to prevent mitochondrial dysfunction in HEPG2 liver cancer cells. (Shin et al., 2009).

RES can inhibit the NOTCH signaling pathway and induce apoptosis in the MOLT-4 T lymphoblastic leukemia cell line. In these cells, RES also inhibited the PI3K/PTEN/AKT/mTORC1/GSK-3 pathway which led to GSK-3beta activation as it was no longer phosphorylated at S9 (Cecchinato et al., 2007). In summary, RES can affect the PI3K/PTEN/AKT/mTORC1, RAS/RAF/MEK/ERK and other pathways which frequently alter gene expression, proliferation, induction of apoptosis, invasion an metastasis.

3. Combining nutraceuticals with signal transduction inhibitors

The effects of combining nutraceuticals such as CUR with PI3K inhibitors have been examined in many cancer models. Co-addition of CUR with the PI3K inhibitor LY294002 increased apoptosis in MCF-7 breast cancer cells. (Kizhakkayil et al., 2010). Likewise, the effects of combining BBR with the dual EGFR/HER2 inhibitor lapatinib. BBR inhibited the lapatinib-resistance of HER2+ breast cancer. The co-treatment resulted in elevated ROS levels. Lapatinib treatment was determined to induce the c-MYC/pro-NRF2 and GSK-3beta signaling pathways in lapatinib-resistant cells which lead to NRF2 stabilization and low levels of ROS. Treatment with BBR increased ROS production and decreased c-MYC expression. This lead to decreased lapatinib-resistance and inhibited cell growth (Zhang et al., 2016a).

RES treatment can also regulate the expression of key genes involved in cell cycle progression. In ovarian cancer cells, RES treatment resulted in decreased cyclin D1. This was determined to occur by RES modulating AKT and subsequent GSK-3beta phosphorylation. In addition, RES also reduced the levels activated ERK1 and ERK2 phosphorylation. Treatment with either PI3K or MEK inhibitors augmented the effects of RES (Vergara et al., 2012).

Various nutraceuticals will have potent anti-oxidant properties and they thus may be suitable for combination with chemotherapeutic drugs to treat cancer cells, including therapy-resistant cancer cells (Prasad et al., 2017; Almomen et al., 2017; Reddyvari et al., 2017; Kumari et al., 2017; Basu and Maier, 2016; Eshwarappa et al., 2015; Babich et al., 2011).

4. Effects of BBR on pancreatic and breast cancer cells

The effects of either BBR or a combination of BBR and different nutraceutical, chemotherapeutic drugs or signal transduction pathway inhibitors were examined in pancreatic and breast cancer cell lines. This scientific approach has clinical relevance as a common goal in cancer therapy is to lower the doses of either chemotherapeutic drugs or signal transduction inhibitors by inclusion of an agent such as a nutraceutical which is normally provided or consumed at low, non-toxic doses. The experiments presented in Figs. 1–5 were all performed the same time.

As controls, the effects of BBR, by itself, on a pancreatic cell line (MIA-PaCA-2) and a breast cancer (MCF-7) cell line are presented in Fig. 1, Panel A. As seen in Panel A, the effects of BBR on MCF-7 and MIA-PaCa-2 cells were similar and IC_{50}s of approximately 700 nM and 1000 nM were observed respectively.

The effects of the nutraceutical genistein, a phytoestrogen which is present in many food sources such as soybeans (Fukutake et al., 1996) were also examined in these same experiments. As seen in Panel B and C, the IC_{50}s of approximately 800 nM and 4000 nM were observed in MIA-PaCa-2 and MCF-7 cells respectively. Both MCF-7 and MIA-PaCa-2 cells are estrogen receptor (ER) positive (Chappell et al., 2013; Guo et al., 2004). Phytoestrogens such as genistein and daidzein have effects on ER + cells which in some cases can stimulate proliferation and in other cases suppress growth (Hsieh et al., 1998). Genistein has been shown to affect ERbeta more than ERalpha (McCarty, 2006). Combining genistein with a suboptimal dose of BBR reduced the berberine IC_{50} from 800 to 60 nM (13.3-fold) in ER + MIA-PaCa-2 cells and from 4000 to 300 (13.3-fold) in ER + MCF-7 cells. Thus, combining genistein with sub-optimal doses of BBR lowered the IC50s for genistein in two ER + cells of different tissue origins.

MIA-PaCa-2 and MCF-7 cells both express the epidermal growth factor receptor (EGFR) (Arnoletti et al., 2004; Nunes-Xavier et al., 2012). When MIA-PaCa-2 or MCF-7 cells were treated with the AG1478 EGFR inhibitor, IC_{50}s of approximately 1000 nM were observed in both cell lines (Fig. 2, Panels A and B). Upon treatment with a suboptimal dose of BBR, the IC_{50} decreased to about 70 nM (14.3-fold) in both MIA-PaCa-2 cells and MCF-7 cells. Thus, co-addition of BBR decreased the concentration of the EGFR inhibitor required to reach the IC_{50} of the EGFR inhibitor in both cell lines.

The protein MEK1 is an important key component of the RAS/RAF/MEK/ERK signaling pathway which is ubiquitously expressed. Upstream *KRAS* is mutated MIA-PaCa-2 and most pancreatic cells and not in MCF-7 breast cancer cells (Fitzgerald et al., 2015; Davis et al., 2014). Upon treatment with the MEK1 inhibitor PD0329501, an IC_{50} of approximately 30 nM was observed in MIA-PaCa-2 cells

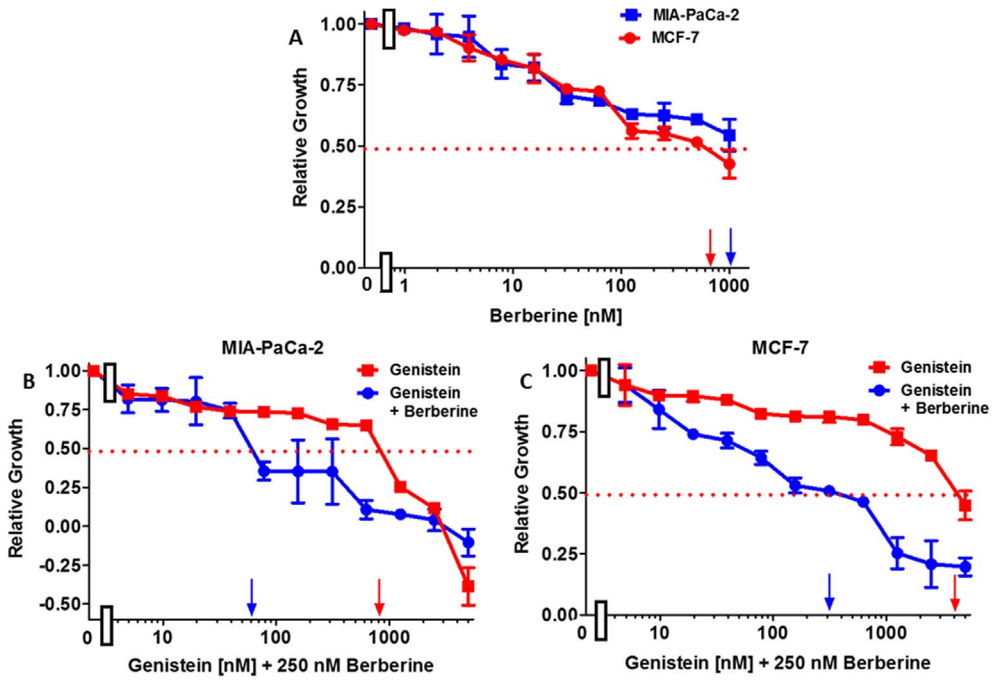

Fig. 1. Effects of the Nutraceuticals Berberine And Genistein on the Proliferation of MIA-PaCa-2 and MCF-7 Cells. MIA-PaCa-2 (blue squares) and MCF-7 (red circles) cells were titrated with different concentrations of BBR (Panel A) or with genistein (red squares) and a sub-optimal dose of berberine (blue circles) (Panels B & C). Arrows on the X-axis indicate where the IC_{50}s can be estimated. In Panel B, the two-tailed *P* value is less than 0.0001 between genistein and genistein and BBR treated MIA-PaCa-2 cells and is considered to be extremely statistically significant. In Panel C, the two-tailed *P* value is less than 0.0001 between genistein and genistein and BBR treated MCF-7 cells and is considered to be extremely statistically significant. All of the experiments indicated in this figure were performed on the same day. These experiments were repeated 3 times and similar results were obtained. (For interpretation of the references to colour in this figure legend, the reader is referred to the web version of this article.)

(Fig. 2, Panel C) and approximately 200 nM in MCF-7 cells (Fig. 2, Panel D). However, upon treatment with a suboptimal dose of BBR, the IC_{50} decreased to about 2 nM (15-fold) in MIA-PaCa-2 cells and 15 nM (13.3-fold) in MCF-7 cells. Thus, co-addition of BBR decreased the concentration of the MEK1 inhibitor required to reach the IC_{50} for the MEK1 inhibitor in both cell lines.

Parthenolide is another natural product that is a sesquiterpene lactone. Parthenolide has been isolated from feverfew and other plants. It has various biochemical targets including NF-kappa-B, histone deacetylases and others (McCubrey et al., 2012a; Hartman et al., 2016). When MIA-PaCa-2 and MCF-7 cells were treated with parthenolide, IC_{50}s of approximately 22 nM and 3 nM were observed respectively (Fig. 3, Panels A and B). When the cells were treated with the suboptimal doses of BBR, the levels of relative growth decreased in both the MIA-PaCa-2 and MCF-7 cells. The IC_{50} for parthenolide dropped from 22 to 0.8 nM (27.5-fold) in MIA-PaCa-2 cells (Panel A) but did not change significantly in MCF-7 cells (Panel B).

The effects of the BCL2 inhibitor ABT737 on MIA-PaCa-2 and MCF-7 cells were examined (Panels C and D respectively). When MIA-PaCa-2 and MCF-7 cells were treated with the ABT737 inhibitor, IC_{50}s of 220 and 40 nM were observed respectively. When MIA-PaCa-2 cells were treated with the BCL2 inhibitor and the suboptimal concentration of BBR (Panel C), the IC_{50} for the BCL2 inhibitor dropped from 220 nM to approximately 8 nM (27.5-fold). In contrast, the addition of the suboptimal dose of BBR (Panel D) did not reduce the IC_{50} of the BCL2 inhibitor in MCF-7 cells, the apparent IC_{50} in the co-addition increased from about 40 nM to 180 nM (Panel D).

The effects of targeting components of the PI3K/PTEN/AKT/mTORC pathway were examined in MIA-PaCa-2 and MCF-7 cells by treating the cells with the PI3K/mTOR dual inhibitor NVP-BE235 and the mTORC1 blocker rapamycin in Fig. 4. MIA-PaCa-2 cells have mutant *KRAS* while MCF-7 cells have mutant *PIK3CA* (McCubrey et al., 2012b, 2012c). These mutations will result in altered PI3K/AKT/mTOR activity. When MIA-PaCa-2 and MCF-7 cells were treated with the dual PI3K/mTOR NVP-BE235 inhibitor, IC_{50}s of approximately 60 nM and 8 nM were observed (Panels A and B respectively). When the cells were treated with the suboptimal concentration of BBR and NVP-BE235, IC_{50}s of 4 nM and 1.3 nM were observed respectively. Thus, BBR reduced the IC_{50}s for NVP-BE235 in both MIA-PaCa-2 and MCF-7 cells (15-fold and 6.3-fold respectively).

The effects of the mTORC1 blocker rapamycin on MIA-PaCa-2 and MCF-7 cells were determined (Panels C and D). When MIA-PaCa-2 or MCF-7 cells were treated with rapamycin, IC_{50}s of approximately 30 nM and 3 nM were observed respectively. When the cells were treated with the suboptimal concentration of BBR and rapamycin, IC_{50}s of 0.08 nM and 0.1 nM were observed respectively. Thus, BBR reduced the IC_{50}s for rapamycin in both MIA-PaCa-2 and MCF-7 cells (375-fold and 30-fold respectively).

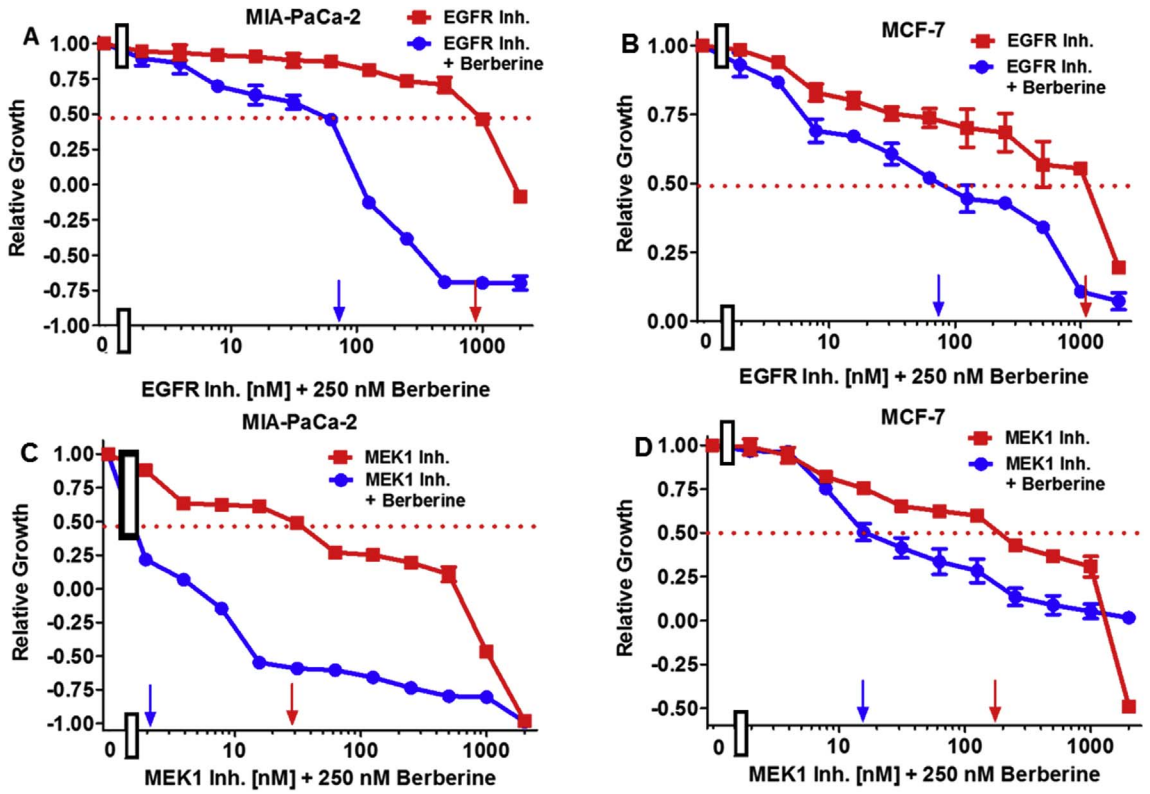

Fig. 2. Effects of EGFR and MEK1 Inhibitors in the Absence and Presence of Suboptimal Doses of BBR on the Proliferation of MIA-PaCa-2 and MCF-7 Cells. MIA-PaCa-2 and MCF-7 cells were titrated with different concentrations of the AG1478 EGFR inhibitor (Panels A and B) or the PD0329501 MEK1 inhibitor (Panels C & D) in the absence (red squares) and presence (blue circles) of sub-optimal doses of berberine. Arrows on the X-axis indicate where the IC_{50}s can be estimated. In Panel A, the two-tailed *P* value is less than 0.0001 between the AG1478 EGFR inhibitor and the AG1478 EGFR inhibitor and BBR-treated MIA-PaCa-2 cells and is considered to be extremely statistically significant. In Panel B, the two-tailed *P* value is less than 0.0001 between the AG1478 EGFR inhibitor and the AG1478 EGFR inhibitor and BBR-treated MCF-7 cells and is considered to be extremely statistically significant. In Panel C, the two-tailed *P* value is less than 0.0001 between the PD0329501 MEK1 inhibitor and the PD0329501 MEK1 inhibitor and BBR-treated MIA-PaCa-2 cells is less than 0.0001 and is considered to be extremely statistically significant. In Panel D, the two-tailed *P* value is less than 0.0001 between the PD0329501 MEK1 inhibitor and the PD0329501 MEK1 inhibitor and BBR-treated MCF-7 cells and is considered to be extremely statistically significant. All of the experiments indicated in this figure were performed on the same day. These experiments were repeated 3 times and similar results were obtained. (For interpretation of the references to colour in this figure legend, the reader is referred to the web version of this article.)

5. Effects of combining BBR with chemotherapeutic drugs on pancreatic cancer cells

The effects of BBR and four different chemotherapeutic drugs on MIA-PaCa-2 cells were examined (Fig. 5). When MIA-PaCa-2 cells were cultured with different doses of doxorubicin, an IC_{50} of approximately 300 nM was observed (Panel A). When these same cells were cultured with doxorubicin and the suboptimal concentration of BBR, the concentration of doxorubicin required to reach the IC_{50} was approximately 40 nM, a reduction of 7.5-fold.

Upon exposure of MIA-PaCa-2 cells to different doses of mitoxantrone, an IC_{50} of approximately 400 nM was observed (Panel B). When these same cells were cultured with mitoxantrone and the suboptimal concentration of BBR, the concentration of mitoxantrone required to reach the IC_{50} was approximately 50 nM, a reduction of 8-fold.

When MIA-PaCa-2 cells were cultured with different doses of docetaxel, an IC_{50} of approximately 18 nM was observed (Panel C). When these same cells were cultured with docetaxel and the suboptimal concentration of BBR, the concentration of docetaxel required to reach the IC_{50} was approximately 0.35 nM, a reduction of 51-fold.

Upon exposure of MIA-PaCa-2 cells to different doses of paclitaxel, an IC_{50} of approximately 0.4 nM was observed (Panel D). When these same cells were cultured with paclitaxel and the suboptimal concentration of BBR, the concentration of paclitaxel required to reach the IC_{50} was approximately 0.02 nM, a reduction of 20-fold. Thus, suboptimal BBR treatments with certain chemotherapeutic drugs would reduce the concentration of the chemotherapeutic drug required to reach the IC_{50} for the chemotherapeutic drug.

6. Effects of suboptimal concentrations of RES and chemotherapeutic drugs on pancreatic cancer cells

This set experiments was performed on a different time than the experiments presented in Figs. 1–5, that is a reason why the titration curves and IC_{50}s presented may be slightly different. As a control, the effect of RES by itself, on MIA-PaCa-2 cells was

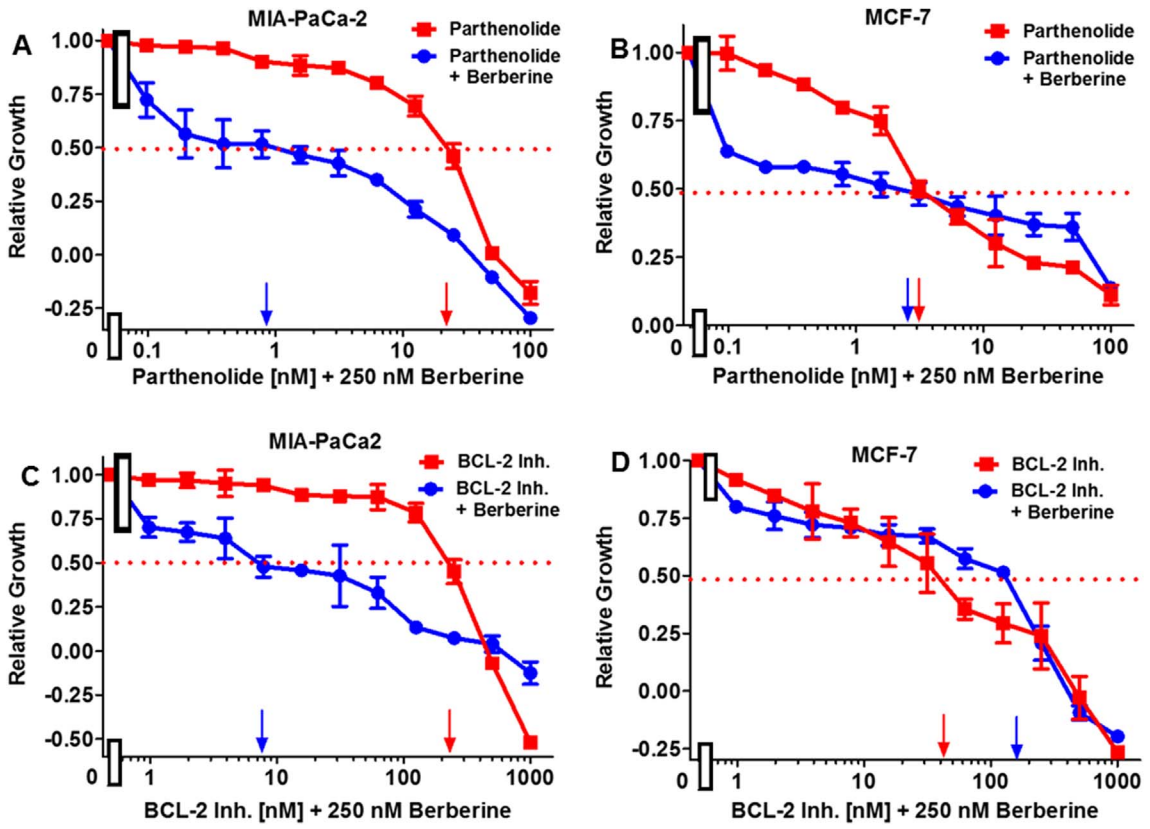

Fig. 3. Effects of Parthenolide and BCL2 Inhibitors in the Absence and Presence of Suboptimal Doses of BBR on the Proliferation of MIA-PaCa-2 and MCF-7 Cells. MIA-PaCa-2 and MCF-7 cells were titrated with different concentrations of the natural product parthenolide (Panels A and B) or the ABT737 BCL2 inhibitor (Panels C & D) in the absence (red squares) and presence (blue circles) of sub-optimal doses of berberine. Arrows on the X-axis indicate where the IC_{50}s can be estimated. In Panel A, the two-tailed *P* value is less than 0.0001 between parthenolide and parthenolide and BBR-treated MIA-PaCa-2 cells and is considered to be extremely statistically significant. In Panel B, the two-tailed *P* value is 1 between parthenolide and parthenolide and BBR-treated MCF-7 cells and is not considered to be statistically significant. In Panel C, the two-tailed *P* value is less than 0.0001 between the ABT737 BCL2 inhibitor and ABT737 BCL2 inhibitor and BBR-treated MIA-PaCa-2 cells and is considered to be extremely statistically significant. In Panel D, the two-tailed *P* value is less than 0.0001 between the ABT737 BCL2 inhibitor and ABT737 BCL2 inhibitor and BBR-treated MCF-7 cells and is considered to be extremely statistically significant. All of the experiments indicated in this figure were performed on the same day. These experiments were repeated 3 times and similar results were obtained. (For interpretation of the references to colour in this figure legend, the reader is referred to the web version of this article.)

examined and an IC_{50} of approximately 35 μM was detected (Fig. 6, Panel A). When the MIA-PaCa-2 cells were treated with chemotherapeutic drug doxorubicin, an IC_{50} of approximately 200 nM was observed (Panel B). Upon culture of the MIA-PaCa-2 cells with doxorubicin and a suboptimal concentration of 12.5 μM RES, the IC_{50} did not decrease.

When the MIA-PaCa-2 cells were treated with chemotherapeutic drug docetaxel, an IC_{50} of approximately 10 nM was observed (Panel C). Upon culture of the MIA-PaCa-2 cells with docetaxel and a suboptimal concentration of 12.5 μM RES, the level of growth detected decreased and the IC_{50} declined slightly from 10 nM to 7 nM, approximately 1.4-fold.

When the MIA-PaCa-2 cells were treated with chemotherapeutic drug mitoxantrone, an IC_{50} of approximately 20 nM was observed (Panel D). Upon culture of the MIA-PaCa-2 cells with mitoxantrone and a suboptimal concentration of 12.5 μM RES, the level of growth detected decreased and the IC_{50} declined from 20 nM to 2 nM, approximately 10-fold. The IC_{50} for mitoxantrone in these experiments was lower than that observed in the experiments presented in Fig. 5. These experiments were performed on different dates These experiments illustrate the importance of performing the drug treatment and drug treatment combined with nutraceuticals at the same time. All the experiments presented in this manuscript where performed in that fashion.

When the MIA-PaCa-2 cells were treated with chemotherapeutic drug 5-fluorouracil (5-FU), an IC_{50} of approximately 4 μM was observed (Panel E). Upon culture of the MIA-PaCa-2 cells with 5-FU and a suboptimal concentration of 12.5 μM RES, the level of growth detected decreased and the IC_{50} declined from 4 μM to 2 μM, approximately 2-fold.

When the MIA-PaCa-2 cells were treated with chemotherapeutic drug cisplatin, an IC_{50} of approximately 100 μM was observed (Panel F). Upon culture of the MIA-PaCa-2 cells with cisplatin and a suboptimal concentration of 12.5 μM RES, the level of growth detected decreased slightly.

When the MIA-PaCa-2 cells were treated with chemotherapeutic drug oxaliplatin, an IC_{50} of approximately 2 μM was observed (Fig. 7, Panel A). Upon culture of the MIA-PaCa-2 cells with oxaliplatin and a suboptimal concentration of 12.5 μM RES, the level of growth detected decreased and the IC_{50} declined from 2 μM to 0.4 μM, approximately 5-fold.

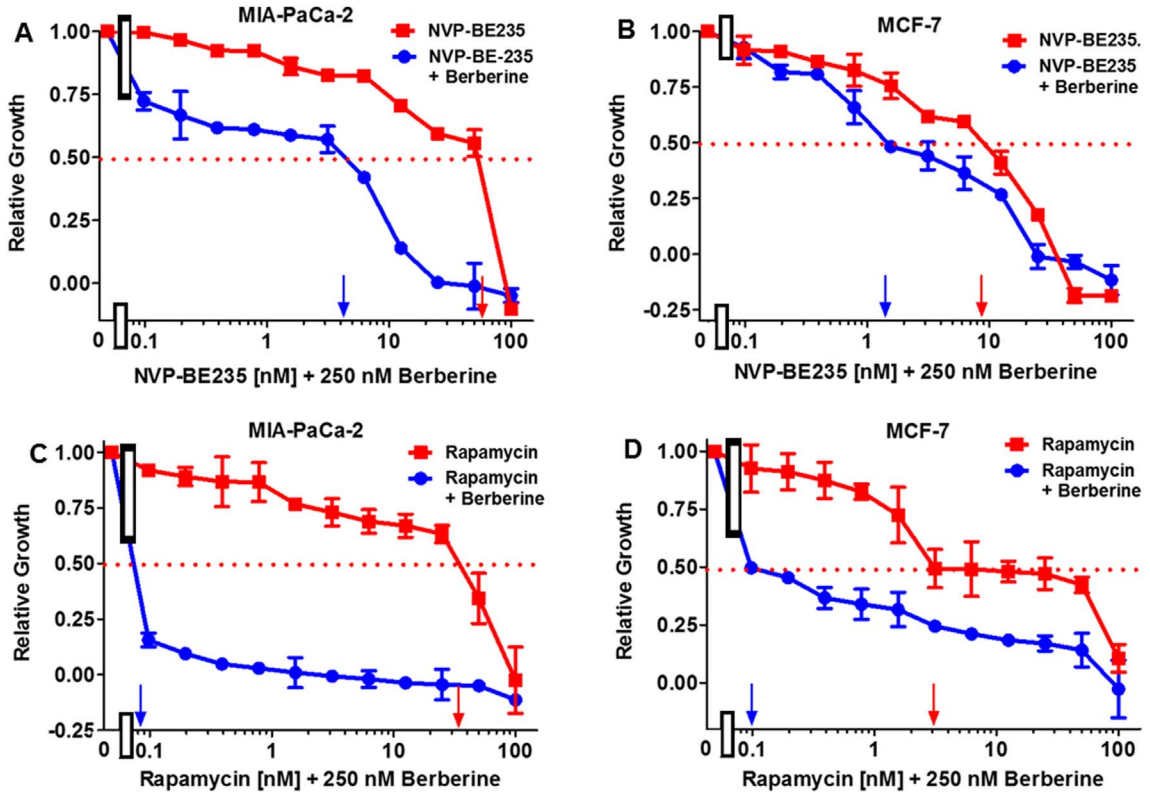

Fig. 4. Effects of PI3K/mTOR Inhibitor and the mTORC1 Blocker Rapamycin in the Absence and Presence of Suboptimal Doses of BBR on the Proliferation of MIA-PaCa-2 and MCF-7 Cells. MIA-PaCa-2 and MCF-7 cells were titrated with different concentrations of the dual PI3K/mTOR inhibitor NVP-BE235 (Panels A and B) or the mTORC1 blocker (Panels C & D) in the absence (red squares) and presence (blue circles) of sub-optimal doses of berberine. Arrows on the X-axis indicate where the IC_{50}s can be estimated. In Panel A, the two-tailed *P* value is less than 0.0001 between the dual PI3K/mTOR inhibitor NVP-BE235 and the dual PI3K/mTOR inhibitor NVP-BE235 and BBR-treated MIA-PaCa-2 cells and is considered to be extremely statistically significant. In Panel B, the two-tailed *P* value is less than 0.0001 between the dual PI3K/mTOR inhibitor NVP-BE235 and the dual PI3K/mTOR inhibitor NVP-BE235 and BBR-treated MCF-7 cells and is considered to be extremely statistically significant. In Panel C, the two-tailed *P* value is less than 0.0001 between the mTORC1 blocker rapamycin and the mTORC1 blocker rapamycin and BBR-treated MIA-PaCa-2 cells and is considered to be extremely statistically significant. In Panel D, the two-tailed *P* value is less than 0.0001 between the mTORC1 blocker rapamycin and the mTORC1 blocker rapamycin and BBR-treated MCF-7 cells and is considered to be extremely statistically significant. All of the experiments indicated in this figure were performed on the same day. (For interpretation of the references to colour in this figure legend, the reader is referred to the web version of this article.)

7. Effects of suboptimal concentrations of RES and signal transduction inhibitors and natural products on pancreatic cancer cells

When the MIA-PaCa-2 cells were treated with the proteasomal inhibitor MG132, an IC_{50} of approximately 10 nM was observed (Fig. 7, Panel B). Upon culture of the MIA-PaCa-2 cells with MG132 and a suboptimal concentration of 12.5 μM RES, the level of growth detected decreased and the IC_{50} declined from 10 nM to 4 nM, approximately 2.5-fold.

When the MIA-PaCa-2 cells were treated with the dual PI3K/mTOR inhibitor NVP-BE235, an IC_{50} of approximately 18 nM was observed (Fig. 7, Panel C). Upon culture of the MIA-PaCa-2 cells with NVP-BE235 and a suboptimal concentration of 12.5 μM RES, the level of growth detected decreased and the IC_{50} declined from 18 nM to 0.08 nM, approximately 225-fold.

When the MIA-PaCa-2 cells were treated with mTORC1 blocker rapamycin, an IC_{50} of approximately 100 nM was observed (Fig. 7, Panel D). Upon culture of the MIA-PaCa-2 cells with rapamycin and a suboptimal concentration of 12.5 μM RES, the level of growth detected decreased and the IC_{50} declined from 100 nM to 0.2 nM, approximately 500-fold. Treatment with rapamycin often yielded different sensitivities on different days This is most likely due to the metabolic state of the cells on different days which resulted in the cells having different sensitivities to rapamycin.

When the MIA-PaCa-2 cells were treated with BBR, an IC_{50} of approximately 3000 nM was observed (Fig. 7, Panel E). Upon culture of the MIA-PaCa-2 cells with BBR and a suboptimal concentration of 12.5 μM RES, the level of growth detected decreased and the IC_{50} declined slightly from 3000 nM to 2000 nM, approximately 1.5-fold.

When the MIA-PaCa-2 cells were treated with CUR, an IC_{50} of approximately 15 μM was observed (Fig. 7, Panel F). Upon culture of the MIA-PaCa-2 cells with CUR and a suboptimal concentration of 12.5 μM RES, the level of growth detected decreased and the IC_{50} declined from 15 μM to 0.15 μM, approximately 100-fold.

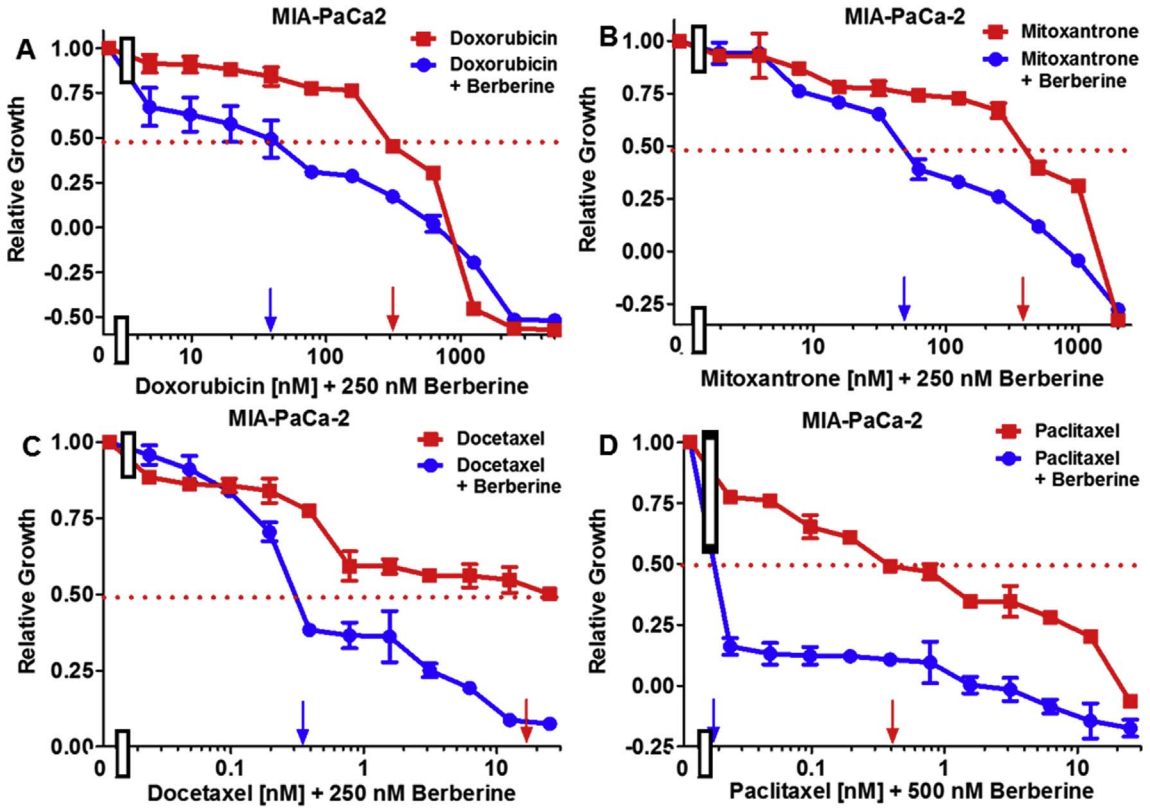

Fig. 5. Effects of Chemotherapeutic Drugs in the Absence and Presence of Suboptimal Doses of BBR on the Proliferation of MIA-PaCa-2 Cells. MIA-PaCa-2 cells were titrated with different concentrations of the chemotherapeutic drugs: Panel A) doxorubicin), Panel B, mitoxantrone, Panel C) docetaxel and Panel D) paclitaxel in the absence (red squares) and presence (blue circles) of sub-optimal doses of berberine. Arrows on the X-axis indicate where the IC_{50}s can be estimated. In Panel A, the two-tailed *P* value is less than 0.0001 between the doxorubicin and the doxorubicin and BBR-treated MIA-PaCa-2 cells and is considered to be extremely statistically significant. In Panel B, the two-tailed *P* value is less than 0.0001 between the mitoxantrone and the mitoxantrone and BBR-treated MIA-PaCa-2 cells and is considered to be extremely statistically significant. In Panel C, the two-tailed *P* value is less than 0.0001 between the docetaxel and the docetaxel and BBR-treated MIA-PaCa-2 cells is less than 0.0001 and is considered to be extremely statistically significant. In Panel D, the two-tailed *P* value is less than 0.0001 between the paclitaxel and the paclitaxel and BBR-treated MIA-PaCa-2 cells and is considered to be extremely statistically significant. All of the experiments indicated in this figure were performed on the same day. (For interpretation of the references to colour in this figure legend, the reader is referred to the web version of this article.)

8. Effects of suboptimal concentrations of CUR and chemotherapeutic drugs on pancreatic cancer cells

As a control, the effects of CUR, by itself, on MIA-PaCa-2 cells were examined and an IC_{50} of approximately 10 μM was detected (Fig. 8, Panel A). When the MIA-PaCa-2 cells were treated with the chemotherapeutic drug doxorubicin, an IC_{50} of approximately 100 nM was observed (Fig. 8, Panel B). Upon culture of the MIA-PaCa-2 cells with doxorubicin and a suboptimal concentration of 5 μM CUR, the amount of growth decreased and the IC_{50} decreased from 100 to 8 nM (12.5-fold).

When the MIA-PaCa-2 cells were treated with the chemotherapeutic drug docetaxel, an IC_{50} of approximately 20 nM was observed (Fig. 8, Panel C). Upon culture of the MIA-PaCa-2 cells with docetaxel and a suboptimal concentration of 5 μM CUR, the amount of growth decreased dramatically and the IC_{50} declined from 20 to 0.4 nM (50-fold).

When the MIA-PaCa-2 cells were treated with the chemotherapeutic drug mitoxantrone, an IC_{50} of approximately 10 nM was observed (Fig. 8, Panel D). Upon culture of the MIA-PaCa-2 cells with mitoxantrone and a suboptimal concentration of 5 μM CUR, the amount of growth decreased and the IC_{50} declined from 10 to 1.5 nM (6.7-fold).

When the MIA-PaCa-2 cells were treated with the chemotherapeutic drug 5FU, an IC_{50} of approximately 8 μM was observed (Fig. 8, Panel E). Upon culture of the MIA-PaCa-2 cells with 5FU and a suboptimal concentration of 5 μM CUR, the amount of growth decreased slightly and the IC_{50} declined from 8 to 4 μM (2-fold).

When the MIA-PaCa-2 cells were treated with the chemotherapeutic drug cisplatin, an IC_{50} of approximately 120 μM was observed (Fig. 8, Panel F). Upon culture of the MIA-PaCa-2 cells with cisplatin and a suboptimal concentration of 5 μM CUR, the amount of growth decreased substantially and the IC_{50} declined dramatically from 120 to 0.4 μM (300-fold).

When the MIA-PaCa-2 cells were treated with the chemotherapeutic drug oxaliplatin, an IC_{50} of approximately 2 μM was observed (Fig. 9, Panel A). Upon culture of the MIA-PaCa-2 cells with oxaliplatin and a suboptimal concentration of 5 μM CUR, the amount of growth decreased substantially and the IC_{50} declined from 2 to 0.3 μM (6.7-fold).

When the MIA-PaCa-2 cells were treated with the chemotherapeutic drug gemcitabine, an IC_{50} of approximately 0.25 nM was

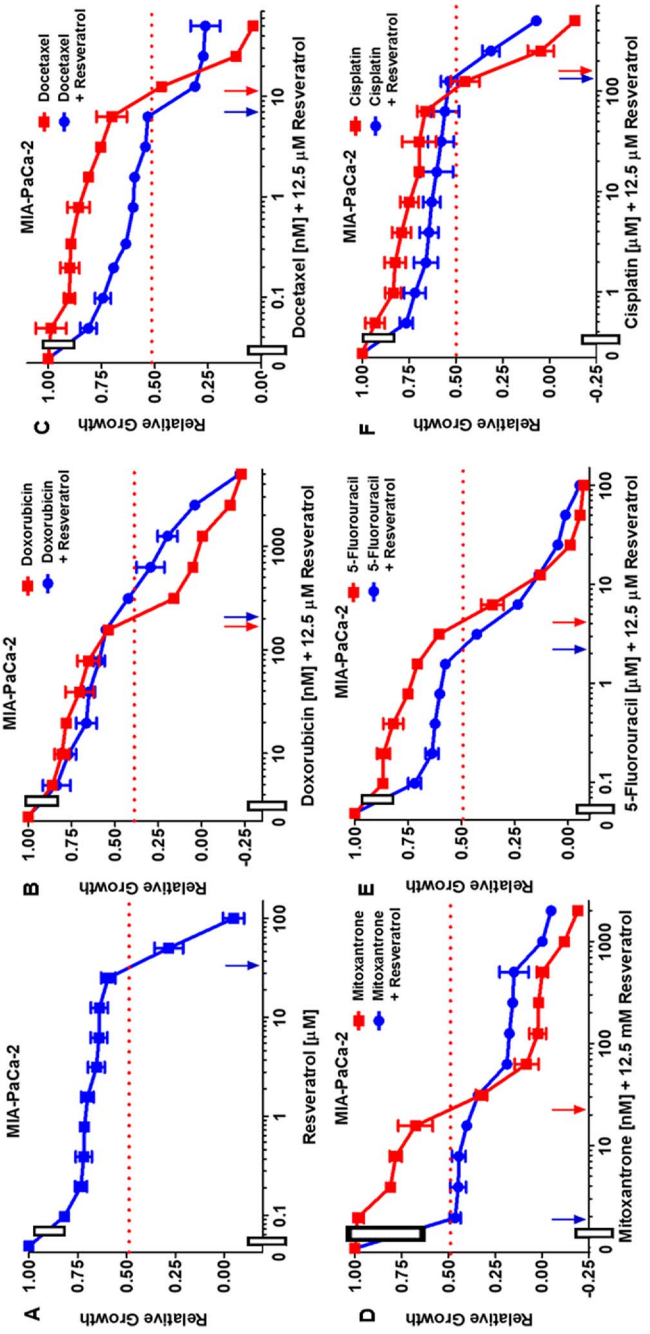

Fig. 6. Effects of RES by Itself and Chemotherapeutic Drugs in the Absence and Presence of Suboptimal Doses of RES on the Proliferation of MIA-PaCa-2 Cells. MIA-PaCa-2 cells were titrated with different concentrations of RES (Panel A) or chemotherapeutic drugs: Panel B) doxorubicin), Panel C, docetaxel, Panel D) mitoxantrone, Panel E) 5-fluorouracil and Panel E) cisplatin in the absence (red squares) and presence (blue circles) of sub-optimal doses of berberine. Arrows on the X-axis indicate where the IC_{50}s can be estimated. In Panel B, the two-tailed *P* value is 0.0036 between the doxorubicin and the doxorubicin and RES-treated MIA-PaCa-2 cells and is considered to be very statistically significant. In Panel C, the two-tailed *P* value is 0.0005 between the docetaxel and the docetaxel and RES-treated MIA-PaCa-2 cells and is considered to be extremely statistical significant. In Panel D, the two-tailed *P* value is less than 0.0001 between the mitoxantrone and the mitoxantrone and RES-treated MIA-PaCa-2 cells and is considered to be extremely statistical significant. In Panel E, the two-tailed *P* value is less than 0.0001 between the 5FU and the 5FU and RES-treated MIA-PaCa-2 cells and is considered to be extremely statistical significant. In Panel F, the two-tailed *P* value is 1 between the cisplatin and the cisplatin and RES-treated MIA-PaCa-2 cells and is not considered to be statistical significant. All of the experiments indicated in this figure were performed on the same day. (For interpretation of the references to colour in this figure legend, the reader is referred to the web version of this article.)

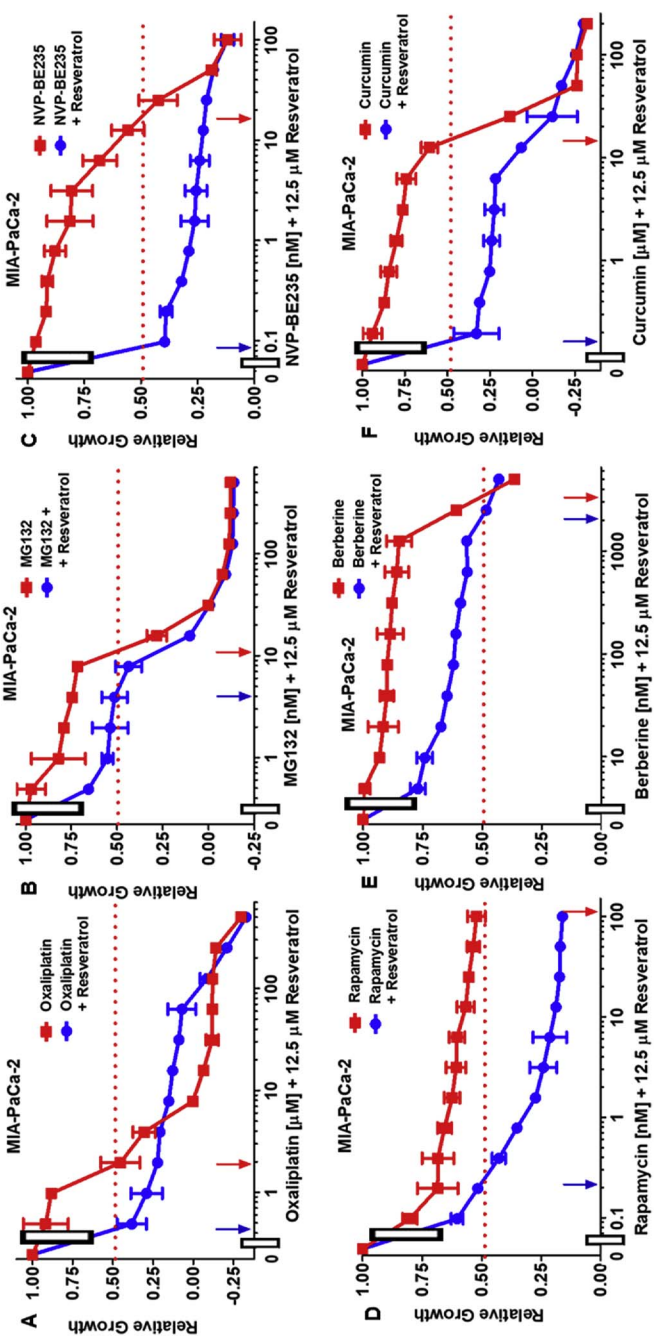

Fig. 7. Effects of Chemotherapeutic Drugs, Signal Transduction Inhibitors and Natural Products in the Absence and Presence of Suboptimal Doses of RES on the Proliferation of MIA-PaCa-2 Cells. MIA-PaCa-2 cells were titrated with different concentrations of: Panel A) oxaliplatin, Panel B) the proteasomal inhibitor MG132, Panel C) the PI3K/Akt inhibitor NVP-BE235, Panel D) the mTORC1 blocker rapamycin, Panel E) BBR or Panel F) CUR in the absence (red squares) and presence (blue circles) of sub-optimal doses of berberine. Arrows on the X-axis indicate where the IC_{50}s can be estimated. In Panel A, the two-tailed *P* value is 0.0003 between the oxaliplatin and the oxaliplatin and RES-treated MIA-PaCa-2 cells and is considered to be extremely statistical significant. In Panel B, the two-tailed *P* value is less 0.0001 between the proteasomal inhibitor MG132 and the proteasomal inhibitor MG132 and RES-treated MIA-PaCa-2 cells and is considered to be extremely statistical significant. In Panel C, the two-tailed *P* value is less 0.0001 between the dual PI3K/mTOR inhibitor NVP-BE235 and the dual PI3K/mTOR inhibitor NVP-BE235 and RES-treated MIA-PaCa-2 cells and is considered to be extremely statistical significant. In Panel D, the two-tailed *P* value is less 0.0001 between the mTORC1 blocker rapamycin and the mTORC1 blocker rapamycin and RES-treated MIA-PaCa-2 cells and is considered to be extremely statistical significant. In Panel E, the two-tailed *P* value is less 0.0001 between the BBR and the BBR and RES-treated MIA-PaCa-2 cells and is considered to be extremely statistical significant. In Panel F, the two-tailed *P* value is less 0.0001 between the CUR and the CUR and RES-treated MIA-PaCa-2 cells and is considered to be extremely statistical significant. (For interpretation of the references to colour in this figure legend, the reader is referred to the web version of this article.)

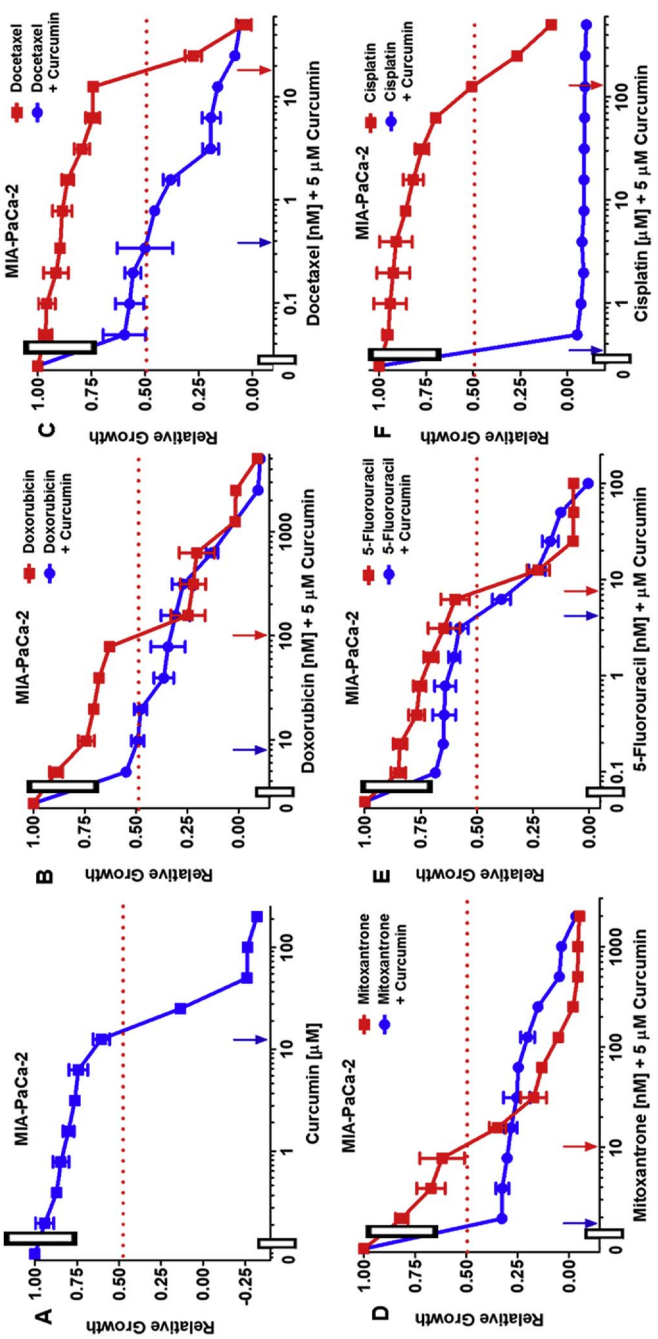

Fig. 8. Effects of CUR by Itself and Chemotherapeutic Drugs in the Absence and Presence of Suboptimal Doses of CUR on the Proliferation of MIA-PaCa-2 Cells. MIA-PaCa-2 cells were titrated with different concentrations of CUR (Panel A) or chemotherapeutic drugs: Panel B) doxorubicin), Panel C, docetaxel, Panel D) mitoxantrone, Panel E) 5FU and Panel E) cisplatin in the absence (red squares) and presence (blue circles) of sub-optimal doses of CUR. Arrows on the X-axis indicate where the IC_{50}s can be estimated. In Panel B, the two-tailed *P* value is less 0.0001 between the doxorubicin and the doxorubicin and CUR-treated MIA-PaCa-2 cells and is considered to be extremely statistical significant. In Panel C, the two-tailed *P* value is less 0.0001 between the docetaxel and the docetaxel and CUR-treated MIA-PaCa-2 cells and is considered to be extremely statistical significant. In Panel D, the two-tailed *P* value is less 0.0002 between the mitoxantrone and the mitoxantrone and CUR-treated MIA-PaCa-2 cells and is considered to be extremely statistical significant. In Panel E, the two-tailed *P* value is 0.0002 between the 5FU and the 5FU and CUR-treated MIA-PaCa-2 cells and is considered to be extremely statistical significant. In Panel F, the two-tailed *P* value is less than 0.0001 between the cisplatin and the cisplatin and CUR-treated MIA-PaCa-2 cells and is considered to be extremely statistical significant. All of the experiments indicated in this figure were performed on the same day. (For interpretation of the references to colour in this figure legend, the reader is referred to the web version of this article.)

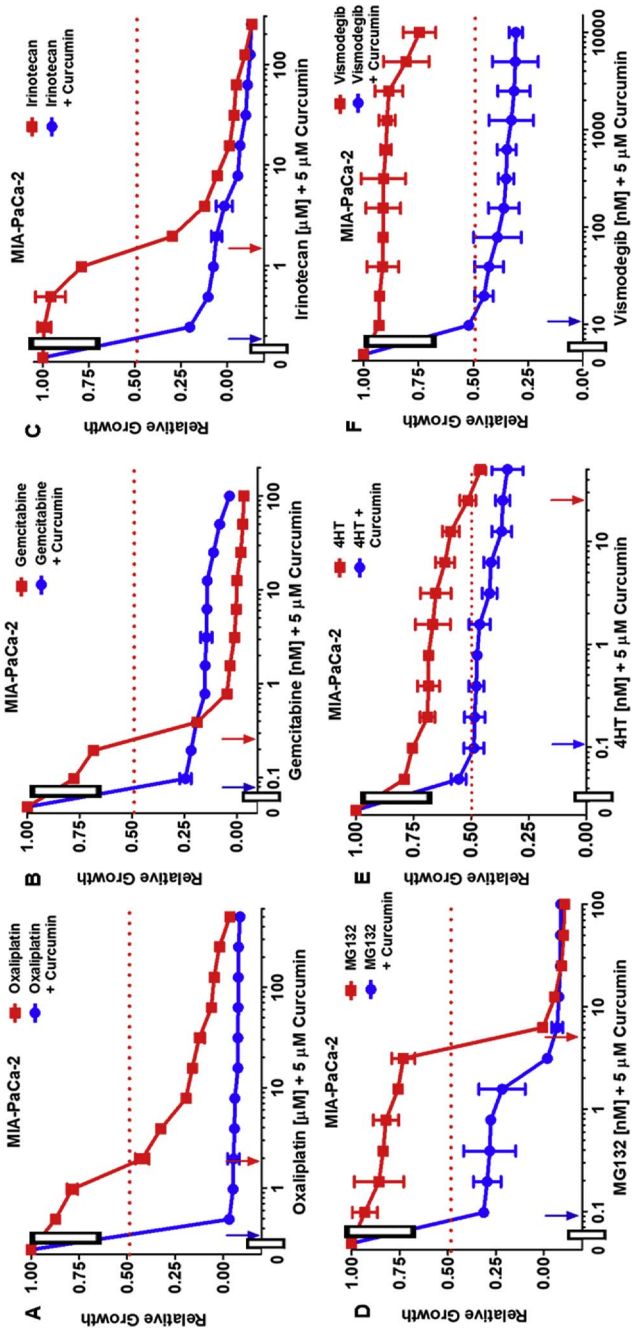

Fig. 9. Effects of Drugs, Natural Products in the Absence and Presence of Suboptimal Doses of CUR on the Proliferation of MIA-PaCa-2 Cells. MIA-PaCa-2 cells were titrated with different concentrations of: Panel A) oxaliplatin, Panel B) gemcitabine, Panel C) irinotecan, Panel D) the proteasomal inhibitor MG132, Panel E) the estrogen receptor antagonist 4 hydroxytamoxifen (4HT) or Panel F) the HH pathway inhibitor vismodegib [antagonist of the smoothened receptor (SMO)] in the absence (red squares) and presence (blue circles) of sub-optimal doses of CUR. Arrows on the X-axis indicate where the IC_{50}s can be estimated. In Panel A, the two-tailed *P* value is less than 0.0001 between the oxaliplatin and the oxaliplatin and CUR-treated MIA-PaCa-2 cells and is considered to be extremely statistical significant. In Panel B, the two-tailed *P* value is less than 0.0001 between the gemcitabine and the gemcitabine and CUR-treated MIA-PaCa-2 cells and is considered to be extremely statistical significant. In Panel C, the two-tailed *P* value is less than 0.0001 between the irinotecan and the irinotecan and CUR-treated MIA-PaCa-2 cells and is considered to be extremely statistical significant. In Panel D, the two-tailed *P* value is less than 0.0001 between the proteasomal inhibitor MG132 and the proteasomal inhibitor MG132 and CUR-treated MIA-PaCa-2 cells and is considered to be extremely statistical significant. In Panel E, the two-tailed *P* value is less than 0.0001 between the ER antagonist 4HT and the 4HT and CUR-treated MIA-PaCa-2 cells and is considered to be extremely statistical significant. (For interpretation of the references to colour in this figure legend, the reader is referred to the web version of this article.)

observed (Fig. 9, Panel B). Upon culture of the MIA-PaCa-2 cells with gemcitabine and a suboptimal concentration of 5 μM CUR, the amount of growth decreased and the IC_{50} declined from 0.25 to 0.07 nM (2.9-fold).

When the MIA-PaCa-2 cells were treated with the chemotherapeutic drug irinotecan, an IC_{50} of approximately 1.5 μM was observed (Fig. 9, Panel C). Upon culture of the MIA-PaCa-2 cells with gemcitabine and a suboptimal concentration of 5 μM CUR, the amount of growth decreased and the IC_{50} declined from 1.5 to 0.2 μM (7.5-fold).

9. Effects of suboptimal concentrations of CUR and signal transduction inhibitors, pharmacological drugs and natural products on pancreatic cancer cells

When the MIA-PaCa-2 cells were treated with the proteasomal inhibitor MG132, an IC_{50} of approximately 5 nM was observed (Fig. 9, Panel D). Upon culture of the MIA-PaCa-2 cells with MG132 and a suboptimal concentration of 5 μM CUR, the amount of growth decreased substantially and the IC_{50} declined significantly from 5 to 0.08 nM (62.5-fold).

When the MIA-PaCa-2 cells were treated with the ER antagonist 4-hydroxytamoxifen (4HT), an IC_{50} of approximately 28 nM was observed (Fig. 9, Panel E). Upon culture of the MIA-PaCa-2 cells with 4HT and a suboptimal concentration of 5 μM CUR, the amount of growth decreased and the IC_{50} declined significantly from 28 to 0.1 nM (280-fold).

When the MIA-PaCa-2 cells were treated with the hedgehog (HH) pathway inhibitor vismodegib, even at concentrations of 10,000 nM, the IC_{50} of was not reached (Fig. 9, Panel F). Upon culture of the MIA-PaCa-2 cells with vismodegib and a suboptimal concentration of 5 μM CUR, the amount of growth decreased substantially and an IC_{50} of approximately 10 nM was observed.

When the MIA-PaCa-2 cells were treated with the anti-malarial drug chloroquine, an IC_{50} of approximately 10 μM was observed (Fig. 10, Panel A). Upon culture of the MIA-PaCa-2 cells with chloroquine and a suboptimal concentration of 5 μM CUR, the amount of growth decreased and the IC_{50} declined substantially from 10 to 0.04 μM (250-fold).

When the MIA-PaCa-2 cells were treated with RES, an IC_{50} of approximately 30 μM was observed (Fig. 10, Panel B). Upon culture of the MIA-PaCa-2 cells with RES and a suboptimal concentration of 5 μM CUR, the amount of growth decreased significantly and the IC_{50} declined substantially from 30 to 0.08 μM (375-fold).

When the MIA-PaCa-2 cells were treated with the dual PI3K/mTOR inhibitor NVP-BE235, an IC_{50} of approximately 20 nM was observed (Fig. 10, Panel C). Upon culture of the MIA-PaCa-2 cells with NVP-BE235 and a suboptimal concentration of 5 μM CUR, the amount of growth decreased substantially and the IC_{50} declined significantly from 20 to 0.08 nM (250-fold).

When the MIA-PaCa-2 cells were treated with the mTORC1 blocker rapamycin, the IC50 was not reached at concentration of rapamycin up to 25 nM (Fig. 10, Panel D). Upon culture of the MIA-PaCa-2 cells with rapamycin and a suboptimal concentration of 5 μM CUR, the amount of growth decreased substantially and the IC_{50} was approximately 0.02 nM.

When the MIA-PaCa-2 cells were treated with BBR, an IC_{50} of approximately 2000 nM was observed (Fig. 10, Panel E). Upon culture of the MIA-PaCa-2 cells with BBR and a suboptimal concentration of 5 μM CUR, the amount of growth decreased substantially and the IC_{50} declined significantly from 2000–2 nM (1000-fold).

When the MIA-PaCa-2 cells were treated with the type-II diabetes drug metformin, the IC_{50} was not reached at concentration up to 10,000 nM (Fig. 10, Panel F). Upon culture of the MIA-PaCa-2 cells with metformin and a suboptimal concentration of 5 μM CUR, the amount of growth decreased substantially and the IC_{50} was approximately 7 nM.

When the MIA-PaCa-2 cells were treated with the AG1478 EGFR inhibitor, an IC_{50} of approximately 2000 nM was observed (Fig. 11, Panel A). Upon culture of the MIA-PaCa-2 cells with the EGFR inhibitor and a suboptimal concentration of 5 μM CUR, the amount of growth decreased and the IC_{50} declined from 2000–250 nM (8-fold).

When the MIA-PaCa-2 cells were treated with the SRC kinase inhibitor dasatinib, an IC_{50} of approximately 18 nM was observed (Fig. 11, Panel B). Upon culture of the MIA-PaCa-2 cells with the SRC inhibitor and a suboptimal concentration of 5 μM CUR, the amount of growth decreased and the IC_{50} declined from 18 to 2 nM (9-fold).

When the MIA-PaCa-2 cells were treated with the natural product *Garcinia cambogia*, an IC_{50} of approximately 100 μg/ml was observed (Fig. 11, Panel C). Upon culture of the MIA-PaCa-2 cells with the *Garcinia cambogia* and a suboptimal concentration of 5 μM CUR, the amount of growth decreased substantially and the IC_{50} declined significantly from 100 to 0.4 μg/ml (250-fold).

When the MIA-PaCa-2 cells (TP53 mutant, gain of function) were treated with the MDM2 inhibitor nutlin-3a, the IC_{50} was not reached even upon 5000 nM treatment (Fig. 11, Panel D). Upon culture of the MIA-PaCa-2 cells with the MDM2 inhibitor and a suboptimal concentration of 5 μM CUR, the amount of growth decreased substantially and an IC_{50} of approximately 4 nM was observed in the combined nutlin-3a and CUR treatment.

10. Conclusions

Natural products/nutraceuticals such as BER, CUR and RES will modulate the activities of the PI3K/PTEN/AKT/mTORC1/GSK-3, RAS/RAF/MEK/ERK and other signaling pathways which can often have suppressive effects on various diverse biochemical processes. We have demonstrated in this manuscript the effects of nutraceuticals on certain pancreatic and breast cancer cells. We have observed that the toxicity of the nutraceuticals or chemotherapeutic drugs can be frequently enhanced by co-addition of a suboptimal does of a different nutraceutical or signal transduction inhibitors. Understanding the ability to combine the effects of these natural compounds with chemotherapeutic drugs could reduce the concentrations of these agents required to achieve effective killing of cancer cells.

Various signaling pathways have been associated with cancer cells and cancer stem cells (CSCs), including, EGFR/HER2, PI3K/PTEN/AKT/mTORC, GSK3, WNT-beta-catenin, HEDGEHOG (HH), JAK/STAT, RSK, BTK and others (Su et al., 2015; Gao et al., 2016;

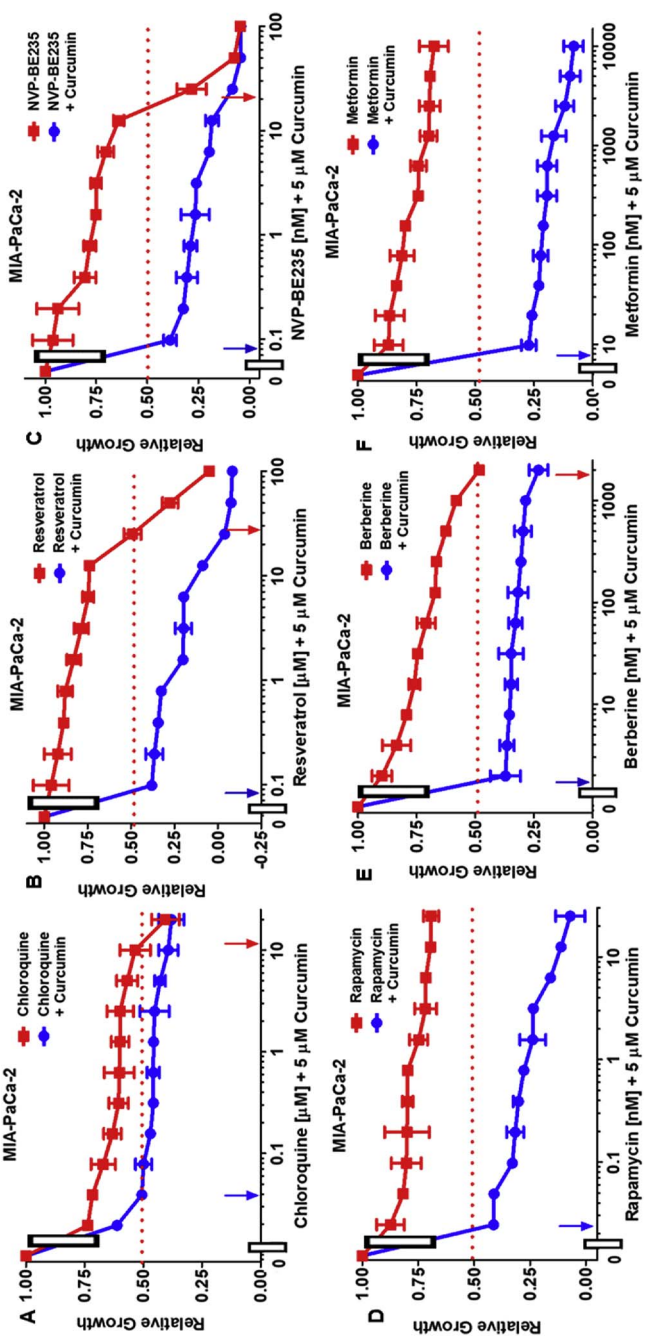

Fig. 10. Effects of Chemotherapeutic Drugs and Signal Transduction Inhibitors in the Absence and Presence of Suboptimal Doses of CUR on the Proliferation of MIA-PaCa-2 Cells. MIA-PaCa-2 cells were titrated with different concentrations of: Panel A) the anti-malarial drug chloroquine, Panel B) RES, Panel C) the PI3K/mTOR inhibitor NVP-BE235, Panel D) the mTORC1 blocker rapamycin, Panel E) BBR or Panel F) the type-II diabetes drug metformin (AMPK activator) in the absence (red squares) and presence (blue circles) of sub-optimal doses of CUR. Arrows on the X-axis indicate where the IC_{50}s can be estimated. In Panel A, the two-tailed *P* value is less than 0.0001 between the anti-malarial drug chloroquine and the anti-malarial drug chloroquine and CUR-treated MIA-PaCa-2 cells and is considered to be extremely statistical significant. In Panel B, the two-tailed *P* value is less than 0.0001 between RES and RES and CUR-treated MIA-PaCa-2 cells and is considered to be extremely statistical significant. In Panel B, the two-tailed *P* value is less than 0.0001 between RES and RES and CUR-treated MIA-PaCa-2 cells and is considered to be extremely statistical significant. In Panel C, the two-tailed *P* value is less than 0.0001 between the PI3K/mTOR inhibitor NVP-BE235 and the PI3K/mTOR inhibitor NVP-BE235 and CUR-treated MIA-PaCa-2 cells and is considered to be extremely statistical significant. In Panel E, the two-tailed *P* value is less than 0.0001 between BBR and BBR and CUR-treated MIA-PaCa-2 cells and is considered to be extremely statistical significant. (For interpretation of the references to colour in this figure legend, the reader is referred to the web version of this article.)

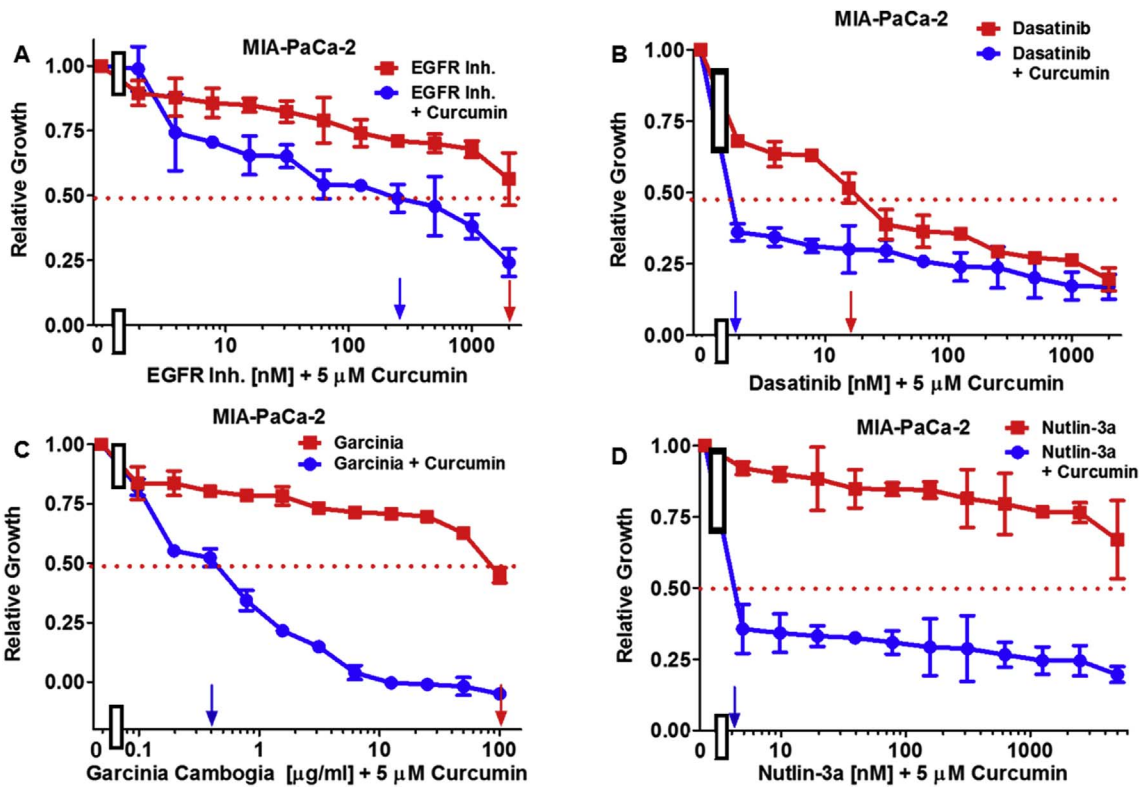

Fig. 11. Effects of Signal Transduction Inhibitors and Natural Products in the Absence and Presence of Suboptimal Doses of CUR on the Proliferation of MIA-PaCa-2 Cells. MIA-PaCa-2 cells were titrated with different concentrations of: Panel A) the AG1478 EGFR inhibitor, Panel B) the SRC kinase inhibitor dasatinib, Panel C) the natural product *Garcinia cambogia* or Panel D) the MDM2 inhibitor nutlin-3a in the absence (red squares) and presence (blue circles) of sub-optimal doses of CUR. Arrows on the X-axis indicate where the IC_{50}s can be estimated. In Panel A, the two-tailed *P* value is less than 0.0001 between the AG1478 EGFR inhibitor and the AG1478 EGFR inhibitor and CUR-treated MIA-PaCa-2 cells and is considered to be extremely statistical significant. In Panel B, the two-tailed *P* value is less than 0.0001 between the SRC kinase inhibitor and the SRC kinase inhibitor and CUR-treated MIA-PaCa-2 cells and considered to be extremely statistical significant. In Panel C, the two-tailed *P* value is less than 0.0001 between the natural product *Garcinia cambogia* and the natural product *Garcinia cambogia* and CUR-treated MIA-PaCa-2 cells and is considered to be extremely statistical significant. (For interpretation of the references to colour in this figure legend, the reader is referred to the web version of this article.)

Mitra et al., 2015; Das et al., 2015).

Various approaches have been designed and evaluated to eliminate cancers. It depends on the cancer and whether certain proteins are expressed. For example EGFR has been considered a target in colorectal cancer (CRC) CSCs (Feng et al., 2016).

Certain EGFR inhibitors affect PI3K signaling in various cancers including lung cancer (Jiang et al., 2016). Novel PI3K inhibitors have shown effects on drug resistant pancreatic cells in part by suppressing epithelial to mesenchymal transition (EMT) and metastasis (Rumman et al., 2016).

Certain novel drugs may target PI3K as well as induce oxidative stress and be effect in therapy resistant head and neck cancers (Prasad et al., 2016). Other drugs such as geridonin and paclitaxel will exhibit synergistic effects and affect the PI3K by the induction of ROS and suppress gastric cancer cells (Wang et al., 2016). Suppression of DNA methyltransferases has been shown to inhibit the resistance to PI3K/mTOR inhibitors (Qian et al., 2015). Certain pan-PI3K inhibitors have been shown to induce WNT signaling in certain cell types such as triple negative breast cancer (TNBC). Combing the PI3K inhibitor with a WNT pathway inhibitor would suppress resistance (Tzeng et al., 2015).

Combining chemotherapy with targeted therapy has also been an active area of investigation and shown to reduce the drug-resistance of certain cancer cells. Combining drugs such as paclitaxel and suppressing TGF-beta will inhibit EMT and breast CSCs (Park et al., 2015).

MEK inhibitors are being evaluated in the treatment of gemcitabine-resistant pancreatic cells in human tumor orthotopic xenograft models (Kawaguchi et al., 2017). The concept of targeting two signaling molecules in a pathway is being examined in melanoma by targeting both BRAF and MEK (Liu et al., 2017). Treatment with MEK inhibitors may enhance the effects of PI3K inhibitors in certain cancer cells by blocking aspects of autophagy (Ren et al., 2016).

Bruton's tyrosine kinase (BTK) is an important kinase involved in B cell development. BTK contains a pleckstrin homology (PH) domain. This domain in phosphatidylinositol (3,4,5)-trisphosphate (PIP3). This results in BTK phosphorylation of phospholipase C. This results in the hydrolyzation of PIP2, a phosphatidylinositol, and generation of inositol triphosphate (IP3) and diacylglycerol (DAG), two key second messengers. Targeting BTK with ibrutinib has been shown to have effects on certain CSCs such as ovarian

CSCs. (Zucha et al., 2015). Combining BCL2 inhibitors with ibrutinib therapy sensitized mantel cell lymphomas (Chiron et al., 2015). Targeting ribosomal S6 kinase (RSK) has been shown to have effects on certain cancers and CSCs by suppressing their drug resistance. RSK lies downstream of the RAF/MEK/ERK pathway (Davies et al., 2015).

mTOR inhibitors have also shown promise in the therapy of thyroid cancers to the BRAF inhibitor vemurafenib (Hanly et al., 2015). Some novel genes responsible for rapalog resistance have been identified by next generation DNA sequencing (Iyer et al., 2012). Point mutations have been found in genes in the mTOR-RHEB pathway in renal cell carcinoma. The cells containing the mutant are still sensitive to rapalogs but they display residual mTORC activity (Ghosh et al., 2015). Certain miRs have been shown to be responsible for the paclitaxel response of breast cancer cells by targeting mTOR (Zhang et al., 2016b). miR-494 targets component of mTOR/p70S6K signaling which results in decreased cisplatin-resistance in ovarian cancer cells (Xu et al., 2015). Recently certain genetic mutations have been determined to confer sensitivity to the rapalog everolimus (Lim et al., 2016).

Quinomycin A, which can bind DNA and has anti-bacterial, anti-tumoral and antiviral properties can affect NOTCH signaling in pancreatic CSCs (Ponnurangam et al., 2016). NOTCH signaling is also important in the development of cisplatin-resistance of osteosarcoma as well as the generation of osteocarcoma CSCs (Yu et al., 2016) NOTCH1 and hypoxia signaling is also important in ovarian CSC (Seo et al., 2016). The STAT3 and NOTCH pathway play key roles in resistance to trastuzumab in gastric cancer (Yang et al., 2015a). Trastuzumab is an antibody which inhibits the effects of the EGFR-related protein HER2 which is often aberrantly expressed in breast, ovarian and gastric cancers.

One of the targets of parthenolide is NF-kappaB. NF-kappaB has been shown to be important in CSCs (Rinkenbaugh et al., 2016). The NF-kappaB pathway is involved in hepatocellular carcinoma (HCC) CSCs which are promoted by osteopontin. (Cao et al., 2015).

MG132 has been one of the most frequently used experimental proteasomal inhibitor. Proteasomal inhibitors will inhibit NF-kappaB and other proteins frequently dysregulated in cancer. Bortezomib is one of the first developed proteasomal inhibitors that has been clinically examined. Proteasomal inhibitors have been examined in various cancers. Bortezomib can affect many processes involved in cell regulation and division, including hypoxia inducible factor-1 (HIF1) signaling, NF-kappaB, NOTCH, telomere homeostasis, DNA repair, apoptosis and autophagy (Grigoreva et al., 2015; Yao et al., 2015; Singha et al., 2015); Thounaojam et al., 2015; Yang et al., 2015b; Li et al., 2015; Fristedt Duvefelt et al., 2015; Han et al., 2015b; Leshchenko et al., 2015; Abdel Malek et al., 2015; Schnerch et al., 2017). Targeting certain kinases such as LYN may be an approach to overcome the bortezomib-resistance of certain mantel cell lymphomas (Kim et al., 2015).

Targeting various components of apoptosis has been an approach examined to suppress cancer growth. Certain BCL2 inhibitors such as venetoclax are being used to treat certain leukemia and other cancers. There are currently at least 71 clinical trials examining the effects of various BCL2 inhibitors. The BCL2 inhibitor ABT-263 has been shown to synergize with chemotherapy in esophageal cancer. This occurred by suppressing pathways associated with stemness (Chen et al., 2015).

Certain BCL2 inhibitors may sensitize certain drug resistant pancreatic cancers to tumor necrosis factor (TNF)-related apoptosis-inducing ligand (TRAIL) treatment (Hari et al., 2015). The effects of BCL2 family inhibitors in combination with CDK inhibitors have been investigated in MCL1-dependent leukemia cells (Choudhary et al., 2015). The effects of BCL2 inhibitors and the cell cycle kinase inhibitor, Oxindole-1 (Ox-1), have been examined in drug resistant AML cells. Polypoid formation is associated with drug resistance and is induced by Ox-1 treatment. The combination was determined to be effective and prevented the development of polyploidy. The critical BCL2-family member was determined to be BCLXL (Zhou et al., 2015b). BCL2 inhibitors could sensitize mantel cell lymphoma cells to acadesine, a nucleoside analogue (Montraveta et al., 2015). Interesting suppressing BCL6 in certain diffuse large B-cell lymphomas will result in activation of BCL2 and BCLXL (Dupont et al., 2016). This phenomenon is referred to as oncogene addiction switching. In this scenario, the B-cell lymphomas should now be sensitive to BCL2 inhibitors. BCL2 inhibitors are also being evaluated in the treatment of certain brain cancers to determine if they can be sensitized to temozolomide (TMZ) and TRAIL (Weyhenmeyer et al., 2016). BCL2 inhibitors have been shown to reverse the vinca alkaloid vinorelbine (VNR) resistance present in certain human lung adenocarcinoma cells. The VNR-resistant cells expressed elevated levels of BCLXL and their suppression resulted with BCL2 inhibitors resulted in sensitivity to vinorelbine (Chiu et al., 2015).

Other BCL2-related proteins may not be sensitive to the more modern BCL2 inhibitors. MCL1 is not sensitive to the effects of ABT-737. Certain nature compounds such as phenylethyl isothiocynate, which is present in watercress, have been shown to target MCL1 which will inhibit drug-resistance and CSCs present in biliary track cancer cells (Li et al., 2016). Flavopiridol is a drug which inhibits cyclin-dependent kinases (CDK) which is used to treat certain leukemia patients. Resistance to flavopiridol can develop in chronic lymphocytic leukemia (CLL) and AML patients. *In vitro* studies have indicated that resistance can result to various factors including prolonged MCL1 stability which was shown to be due to ERK activation (Yeh et al., 2015).

Metformin is an important drug in the treatment of type-II diabetics. It may also have certain anti-cancer effects and suppress CSC. It has been shown that metformin represses bladder cancer progression by inhibiting COX2/PGE2/STAT3 signaling which suppresses bladder CSC repopulation (Liu et al., 2016). Combining metformin and temozomide will inhibit glioma and glioma CSCs (Yu et al., 2015).

The cyclooxygenase inhibitor aspirin has been shown to have effects on pancreatic cancer CSCs. Aspirin sensitized pancreatic cancer CSCs which were resistant to gemcitabine (Zhang et al., 2015).

An additional stress related signaling molecule which is involved in drug transporters, drug-resistance, aerobic glycolysis activity, autophagy and CSCs and is a stress-related molecule is caveolin-1. It also interacts with various stress signals such as AMP-protein kinase which is a target of metformin (Wang et al., 2015). Clearly metabolism plays critical roles in CSC generation and survival (Zhong et al., 2015). Mitochondrial mass as also been associated with CSCs (Farnie et al., 2015). Many nutraceuticals may target aspects of metabolism which are important in cancer cell proliferation as well as CSC generation and survival.

10.1. Materials and methods

Tissue Culture and Treatment of Cells with Signal Transduction Inhibitors and Doxorubicin. Tissue culture medium was obtained from Invitrogen (Carlsbad, CA, USA). Nutraceuticals, chemotherapeutic drugs, signal transduction inhibitors were purchased from either Sigma-Aldrich (Saint Louis, MO, USA) or Selleckchem (Houston, TX USA). MIA-PaCa-2 and MCF-7 cells were titrated with the different nutraceuticals, signal transduction inhibitors, chemotherapeutic and other drugs as described (Chappell et al., 2013; Abrams et al., 2017). Statistical analysis was performed using GraphPad Prism.

Conflicts of interest

The authors declare that they have no conflicts of interest with publication of this manuscript.

Acknowledgements

JAM, SLA and KL were supported in part by a grant from East Carolina University Grants (#111104 and #111110-668715-0000). MC was supported in part by grants to the CNR and from the Italian Ministry of Economy and Finance for the Project FaReBio di Qualita and the Associazione Italiana per la Ricerca sul Cancro (#18394), LC and SR were supported in part by grants from: Intesa San Paolo Foundation. AMM was supported in part by grants from: MIUR FIRB 2011 (RBAP11ZJFA_001). ML and SC were supported in part by a Lega Italiana per la Lotta contro i Tumori grant. DR and AG were supported in part from the Polish National Science Center grant number UMO-2015/19/B/NZ1/00332.

References

Abdel-Aleem, G.A., Khaleel, E.F., Mostafa, D.G., Elberier, L.K., 2016. Neuroprotective effect of resveratrol against brain ischemia reperfusion injury in rats entails reduction of DJ-1 protein expression and activation of PI3K/Akt/GSK3b survival pathway. Arch. Physiol. Biochem. 122, 200–213.
Abdel Malek, M.A., Jagannathan, S., Malek, E., Sayed, D.M., Elgammal, S.A., Abd El-Azeem, H.G., Thabet, N.M., Driscoll, J.J., 2015. Molecular chaperone GRP78 enhances aggresome delivery to autophagosomes to promote drug resistance in multiple myeloma. Oncotarget 6, 3098–3110.
Abrams, S.L., Ruvolo, P.P., Ruvolo, V.R., Ligresti, G., Martelli, A.M., Cocco, L., Ratti, S., Tafuri, A., Steelman, L.S., Candido, S., Libra, M., McCubrey, J.M., 2017. Targeting signaling and apoptotic pathways involved in chemotherapeutic drug-resistance of hematopoietic cells. Oncotarget (in press).
Aditi, L.G., Dawson, T.R., Wente, S.R., 2016. An amyotrophic lateral sclerosis-linked mutation in GLE1 alters the cellular pool of human Gle1 functional isoforms. Adv. Biol. Regul. 62, 25–36.
Almomen, S.M., Guan, Q., Liang, P., Yang, K., Sidiqi, A.M., Levin, A., Du, C., 2017. Daily intake of grape powder prevents the progression of kidney disease in obese type 2 diabetic ZSF1 rats. Nutrients 9, 345.
Anderson, K.E., Juvin, V., Clark, J., Stephens, L.R., Hawkins, P.T., 2016. Investigating the effect of arachidonate supplementation on the phosphoinositide content of MCF10a breast epithelial cells. Adv. Biol. Regul. 62, 18–24.
Arnoletti, J.P., Buchsbaum, D.J., Huang, Z.Q., Hawkins, A.E., Khazaeli, M.B., Kraus, M.H., Vickers, S.M., 2004. Mechanisms of resistance to Erbitux (anti-epidermal growth factor receptor) combination therapy in pancreatic adenocarcinoma cells. J. Gastrointest. Surg. 8, 960–969.
Babich, H., Schuck, A.G., Weisburg, J.H., Zuckerbraun, H.L., 2011. Research strategies in the study of the pro-oxidant nature of polyphenol nutraceuticals. J. Toxicol. 467305 doi: 1155/2011/467305.
Baer, R., Cintas, C., Therville, N., Guillermet-Guibert, J., 2015. Implication of PI3K/Akt pathway in pancreatic cancer: when PI3K isoforms matter? Adv. Biol. Regul. 59, 19–35.
Banfic, H., Crljen, V., Lukinovic-Skudar, V., Dembitz, V., Lalic, H., Bedalov, A., Visnjic, D., 2016. Inositol pyrophosphates modulate cell cycle independently of alteration in telomere length. Adv. Biol. Regul. 60, 22–28.
Barker, C.J., Li, L., Köhler, M., Berggren, P.O., 2015. β-Cell Ca (2+) dynamics and function are compromised in aging. A. Biol. Regul. 57, 112–119.
Basu, P., Maier, C., 2016. In vitro Antioxidant activities and polyphenol contents of seven commercially available fruits. Pharmacogn. Res. 8, 258–264.
Beretta, M., Bauer, M., Hirsch, E., 2015. PI3K signaling in the pathogenesis of obesity: the cause and the cure. Adv. Biol. Regul. 58, 1–15.
Bhowmik, D., Das, S., Hossain, M., Haq, L., Kumar, G.S., 2012. Biophysical characterization of the strong stabilization of the RNA triplex poly(U)·poly(A)∗poly(U) by 9-O-(??-amino) alkyl ether berberine analogs. PLoS One 7, e37939.
Bradshaw, R.A., Pundavela, J., Biarc, J., Chalkley, R.J., Burlingame, A.L., Hondermarck, H., 2015. NGF and ProNGF: regulation of neuronal and neoplastic responses through receptor signaling. Adv. Biol. Regul. 58, 16–27.
Campa, C.C., Hirsch, E., 2017. Rab11 and phosphoinositides: a synergy of signal transducers in the control of vesicular trafficking. Adv. Biol. Regul. 63, 132–139.
Cao, L., Fan, X., Jing, W., Liang, Y., Chen, R., Liu, Y., Zhu, M., Jia, R., Wang, H., Zhang, X., Zhang, Y., Zhou, X., Zhao, J., Guo, Y., 2015. Osteopontin promotes a cancer stem cell-like phenotype in hepatocellular carcinoma cells via an integrin-NF-kappaB-HIF-1alpha pathway. Oncotarget 6, 6627–6640.
Cariello, M., Augello, G., Cimiano, A., Emma, M.R., Balsas, D., Azolane, A., McCubrey, J.A., Montalvo, G., 2017. Pivotal roles of glycogen synthase-3 in hepatocellular carcinoma. Adv. Boil Regal 65, 59–76.
Carman, G.M., Han, G.S., 2017. Phosphatidate phosphatase regulates membrane phospholipid synthesis via phosphatidylserine synthase. Adv. Biol. Regul. 16 pii: S2212–4926(17)30129X.
Carroll, B., Donaldson, J.C., Obeid, L., 2015. Sphingolipids in the DNA damage response. Adv. Biol. Regul. 58, 38–52.
Cecchinato, V., Chiaramonte, R., Nizzardo, M., Cristofaro, B., Basile, A., Sherbet, G.V., Comi, P., 2007. Resveratrol-induced apoptosis in human T-cell acute lymphoblastic leukaemia MOLT-4 cells. Biochem. Pharmacol. 74, 1568–1574.
Cervello, M., Augello, G., Cusimano, A., Emma, M.R., Balasus, D., Azzolina, A., McCubrey, J.A., Montalto, G., 2017. Pivotal roles of glycogen synthase-3 in hepatocellular carcinoma. Adv. Biol. Regul. 65, 59–76.
Chappell, W.H., Abrams, S.L., Lertpiriyapong, K., Fitzgerald, T.L., Martelli, A.M., Cocco, L., Rakus, D., Gizak, A., Terrian, D., Steelman, L.S., McCubrey, J.A., 2016. Novel roles of androgen receptor, epidermal growth factor receptor, TP53, regulatory RNAs, NF-kappa-B, chromosomal translocations, neutrophil associated gelatinase, and matrix metalloproteinase-9 in prostate cancer and prostate cancer stem cells. Adv. Biol. Regul. 60, 64–87.
Chappell, W.H., Abrams, S.L., Stadelman, K.M., LaHair, M.M., Franklin, R.A., Cocco, L., Evangelisti, C., Chiarini, F., Martelli, A.M., Steelman, L.S., McCubrey, J.A., 2013. Increased NGAL (Lnc2) expression after chemotherapeutic drug treatment. Adv. Biol. Regul. 53, 146–155.
Chen, Q., Song, S., Wei, S., Liu, B., Honjo, S., Scott, A., Jin, J., Ma, L., Zhu, H., Skinner, H.D., Johnson, R.L., Ajani, J.A., 2015. ABT-263 induces apoptosis and synergizes with chemotherapy by targeting stemness pathways in esophageal cancer. Oncotarget 6, 25883–25896.
Chiron, D., Dousset, C., Brosseau, C., Touzeau, C., Maiga, S., Moreau, P., Pellat-Deceunynck, C., Le Gouill, S., Amiot, M., 2015. Biological rational for sequential targeting of Bruton tyrosine kinase and Bcl-2 to overcome CD40-induced ABT-199 resistance in mantle cell lymphoma. Oncotarget 6, 8750–8759.
Chiu, W.H., Su, W.C., Li, C.L., Chen, C.L., Lin, C.F., 2015. An increase in glucosylceramide synthase induces Bcl-xL-mediated cell survival in vinorelbine-resistant lung

adenocarcinoma cells. Oncotarget 6, 20513–20524.
Choudhary, G.S., Tat, T.T., Misra, S., Hill, B.T., Smith, M.R., Almasan, A., Mazumder, S., 2015. Cyclin E/Cdk2-dependent phosphorylation of Mcl-1 determines its stability and cellular sensitivity to BH3 mimetics. Oncotarget 6, 16912–16925.
Coant, N., Sakamoto, W., Mao, C., Hannun, Y.A., 2017. Ceramidases, roles in sphingolipid metabolism and in health and disease. Adv. Biol. Regul. 63, 122–131.
Cocco, L., Manzoli, L., Faenza, I., Ramazzotti, G., Yang, Y.R., McCubrey, J.A., Suh, P.G., Follo, M.Y., 2016. Modulation of nuclear PI-PLCbeta1 during cell differentiation. Adv. Biol. Regul. 60, 1–5.
Cordell, G.A., Quinn-Beattie, M.L., Farnsworth, N.R., 2001. The potential of alkaloids in drug discovery. Phytother. Res. 15, 183–205.
Cusimano, A., Balasus, D., Azzolina, A., Augello, G., Emma, M.R., Di Sano, C., Gramignoli, R., Strom, S.C., McCubrey, J.A., Montalto, G., Cervello, M., 2017. Oleocanthal exerts antitumor effects on human liver and colon cancer cells through ROS generation. Int. J. Oncol. 51, 533–544.
Das, S., Rachagani, S., Torres-Gonzalez, M.P., Lakshmanan, I., Majhi, P.D., Smith, L.M., Wagner, K.U., Batra, S.K., 2015. Carboxyl-terminal domain of MUC16 imparts tumorigenic and metastatic functions through nuclear translocation of JAK2 to pancreatic cancer cells. Oncotarget 6, 5772–5787.
Davies, A.H., Reipas, K., Hu, K., Berns, R., Firmino, N., Stratford, A.L., Dunn, S.E., 2015. Inhibition of RSK with the novel small-molecule inhibitor LJI308 overcomes chemoresistance by eliminating cancer stem cells. Oncotarget 6, 20570–20577.
Davis, N.M., Sokolosky, M., Stadelman, K., Abrams, S.L., Libra, M., Candido, S., Nicoletti, F., Polesel, J., Maestro, R., D'Assoro, A., Drobot, L., Rakus, D., Gizak, A., Laidler, P., Dulińska-Litewka, J., Basecke, J., Mijatovic, S., Maksimovic-Ivanic, D., Montalto, G., Cervello, M., Fitzgerald, T.L., Demidenko, Z., Martelli, A.M., Cocco, L., Steelman, L.S., McCubrey, J.A., 2014. Deregulation of the EGFR/PI3K/PTEN/Akt/mTORC1 pathway in breast cancer: possibilities for therapeutic intervention. Oncotarget 5 4603–450.
Diaz-Gerevini, G.T., Repossi, G., Dain, A., Tarres, M.C., Das, U.N., Eynard, A.R., 2016. Beneficial action of resveratrol: how and why? Nutrition 32, 174–178.
Dupont, T., Yang, S.N., Patel, J., Hatzi, K., Malik, A., Tam, W., Martin, P., Leonard, J., Melnick, A., Cerchietti, L., 2016. Selective targeting of BCL6 induces oncogene addiction switching to BCL2 in B-cell lymphoma. Oncotarget 7, 3520–3532.
Dusaban, S.S., Brown, J.H., 2015. PLCε mediated sustained signaling pathways. Adv. Biol. Regul. 57, 17–23.
Ebenezer, D.L., Fu, P., Suryadevara, V., Zhao, Y., Natarajan, V., 2017. Epigenetic regulation of pro-inflammatory cytokine secretion by sphingosine 1-phosphate (S1P) in acute lung injury: role of S1P lyase. Adv. Biol. Regul. 63, 156–166.
Erneux, C., Ghosh, S., Koenig, S., 2016. Inositol(1,4,5)P3 3-kinase isoenzymes: catalytic properties and importance of targeting to F-actin to understand function. Adv. Biol. Regul. 60, 135–143.
Eshwarappa, R.S., Iyer, S., Subaramaihha, S.R., Richard, S.A., Dhananjaya, B.L., 2015. Antioxidant activities of ficus glomerata (moraceae) leaf gall extracts. Pharmacogn. Res. 7, 114–120.
Falasca, M., Ferro, R., 2016. Role of the lysophosphatidylinositol/GPR55 axis in cancer. Adv. Biol. Regul. 60, 88–93.
Farnie, G., Sotgia, F., Lisanti, M.P., 2015. High mitochondrial mass identifies a sub-population of stem-like cancer cells that are chemo-resistant. Oncotarget 6, 30472–30486.
Feng, Y., Gao, S., Gao, Y., Wang, X., Chen, Z., 2016. Anti-EGFR antibody sensitizes colorectal cancer stem-like cells to Fluorouracil-induced apoptosis by affecting autophagy. Oncotarget 7, 81402–81409.
Fields, A.P., Justilien, V., Murray, N.R., 2016. The chromosome 3q26 OncCassette: a multigenic driver of human cancer. Adv. Biol. Regul. 60, 47–63.
Fitzgerald, T.L., Lertpiriyapong, K., Cocco, L., Martelli, A.M., Libra, M., Candido, S., Montalto, G., Cervello, M., Steelman, L., Abrams, S.L., McCubrey, J.A., 2015. Roles of EGFR and KRAS and their downstream signaling pathways in pancreatic cancer and pancreatic cancer stem cells. Adv. Biol. Regul. 59, 65–81.
Fristedt Duvefelt, C., Lub, S., Agarwal, P., Arngarden, L., Hammarberg, A., Maes, K., Van Valckenborgh, E., Vanderkerken, K., Jernberg Wiklund, H., 2015. Increased resistance to proteasome inhibitors in multiple myeloma mediated by cIAP2–implications for a combinatorial treatment. Oncotarget 6, 20621–20635.
Fukutake, M., Takahashi, M., Ishida, K., Kawamura, H., Sugimura, T., Wakabayashi, K., 1996. Quantification of genistein and genistin in soybeans and soybean products. Food Chem. Toxicol. 34, 457–461.
Gao, M., Kong, Y., Yang, G., Gao, L., Shi, J., 2016. Multiple myeloma cancer stem cells. Oncotarget 7, 35466–35477.
Gatto, B., Sanders, M.M., Yu, C., Wu, H.Y., Makhey, D., LaVoie, E.J., Liu, L.F., 1996. Identification of topoisomerase I as the cytotoxic target of the protoberberine alkaloid coralyne. Cancer Res. 56, 2795–2800.
Geck, R.C., Toker, A., 2016. Nonessential amino acid metabolism in breast cancer. Adv. Biol. Regul. 62, 11–17.
Ghim, J., Chelakkot, C., Bae, Y.S., Suh, P.G., Ryu, S.H., 2016. Accumulating insights into the role of phospholipase D2 in human diseases. Adv. Biol. Regul. 61, 42–46.
Ghosh, A.P., Marshall, C.B., Coric, T., Shim, E.H., Kirkman, R., Ballestas, M.E., Ikura, M., Bjornsti, M.A., Sudarshan, S., 2015. Point mutations of the mTOR-RHEB pathway in renal cell carcinoma. Oncotarget 6, 17895–17910.
Giudici, M.L., Clarke, J.H., Irvine, R.F., 2016. Phosphatidylinositol 5-phosphate 4-kinase γ (PI5P4Kγ), a lipid signalling enigma. Adv. Biol. Regul. 61, 47–50.
Gizak, A., Pirog, M., Rakus, D., 2012. Muscle FBPase binds to cardiomyocyte mitochondria under glycogen synthase kinase-3 inhibition or elevation of cellular Ca2+ level. FEBS Lett. 586, 13–19.
Gowda, C., Soliman, M., Kapadia, M., Ding, Y., Payne, K., Dovat, S., 2017a. Casein kinase II (CK2), glycogen synthase Kinase-3 (GSK-3) and ikaros mediated regulation of leukemia. Adv. Bio.l Regul. 65, 16–25.
Gowda, C., Song, C., Kapadia, M., Payne, J.L., Hu, T., Ding, Y., Dovat, S., 2017b. Regulation of cellular proliferation in acute lymphoblastic leukemia by Casein Kinase II (CK2) and Ikaros. Adv. Biol. Regul. 63, 71–80.
Grigoreva, T.A., Tribulovich, V.G., Garabadzhiu, A.V., Melino, G., Barlev, N.A., 2015. The 26S proteasome is a multifaceted target for anti-cancer therapies. Rev. Oncotarget 6, 24733–24749.
Guidetti, G.F., Canobbio, I., Torti, M., 2015. PI3K/Akt in platelet integrin signaling and implications in thrombosis. Adv. Biol. Regul. 59, 36–52.
Guo, J.M., Xiao, B.X., Dai, D.J., Liu, Q., Ma, H.H., 2004. Effects of daidzein on estrogen-receptor-positive and negative pancreatic cancer cells in vitro. World J. Gastroenterol 10, 860–863.
Halicka, H.D., Zhao, H., Li, J., Lee, Y.S., Hsieh, T.C., Wu, J.M., Darzynkiewicz, Z., 2012. Potential anti-aging agents suppress the level of constitutive mTOR- and DNA damage-signaling. Aging (Albany NY) 4, 952–965.
Han, B., Yao, W., Oh, Y.T., Tong, J.S., Li, S., Deng, J., Yue, P., Khuri, F.R., Sun, S.Y., 2015a. The novel proteasome inhibitor carfilzomib activates and enhances extrinsic apoptosis involving stabilization of death receptor 5. Oncotarget 6, 17532–17542.
Han, G., Xia, J., Gao, J., Inagaki, Y., Tang, W., Kokudo, N., 2015b. Anti-tumor effects and cellular mechanisms of resveratrol. Drug Discov. Ther. 9, 1–12.
Hanly, E.K., Bednarczyk, R.B., Tuli, N.Y., Moscatello, A.L., Halicka, H.D., Li, J., Geliebter, J., Darzynkiewicz, Z., Tiwari, R.K., 2015. mTOR inhibitors sensitize thyroid cancer cells to cytotoxic effect of vemurafenib. Oncotarget 6, 39702–39713.
Hari, Y., Harashima, N., Tajima, Y., Harada, M., 2015. Bcl-xL inhibition by molecular-targeting drugs sensitizes human pancreatic cancer cells to TRAIL. Oncotarget 6, 41902–41915.
Hartman, M.L., Talar, B., Sztiller-Sikorska, M., Nejc, D., Czyz, M., 2016. Parthenolide induces MITF-M downregulation and senescence in patient-derived MITF-M high melanoma cell populations. Oncotarget 7, 9026–9040.
Hatch, A.J., Odom, A.R., York, J.D., 2017. Inositol phosphate multikinase dependent transcriptional control. Adv. Biol. Regul. 64, 9–19.
Hayashi, Y., Homma, K., Ichijo, H., 2016. SOD1 in neurotoxicity and its controversial roles in SOD1 mutation-negative ALS. Adv. Biol. Regul. 60, 95–104.
Hermida, M.A., Dinesh Kumar, J., Leslie, N.R., 2017. GSK3 and its interactions with the PI3K/AKT/mTOR signalling network. Adv. Biol. Regul. 65, 5–15.
Hsieh, C.Y., Santell, R.C., Haslam, S.Z., Helferich, W.G., 1998. Estrogenic effects of genistein on the growth of estrogen receptor-positive human breast cancer (MCF-7) cells in vitro and in vivo. Cancer Res. 58, 3833–3838.
http://www.grandviewresearch.com/industry-analysis/turmeric-extract-curcumin-market.
http://www.nutraingredients.com/Markets-and-Trends/US-dominates-global-resveratrol-market.
Huang, L.S., Natarajan, V., 2015. Sphingolipids in pulmonary fibrosis. Adv. Biol. Regul. 57, 55–63.
Iyer, G., Hanrahan, A.J., Milowsky, M.I., Al-Ahmadie, H., Scott, S.N., Janakiraman, M., Pirun, M., Sander, C., Socci, N.D., Ostrovnaya, I., Viale, A., Heguy, A., Peng, L., Chan, T.A., Bochner, B., Bajorin, D.F., Berger, M.F., Taylor, B.S., Solit, D.B., 2012. Genome sequencing identifies a basis for everolimus sensitivity. Science 338, 221.

Jahan, S., Davie, J.R., 2015. Protein arginine methyltransferases (PRMTs): role in chromatin organization. Adv. Biol. Regul. 57, 173–184.
Jhanwar, S.C., 2015. Genetic and epigenetic pathways in myelodysplastic syndromes: a brief overview. Adv. Biol. Regul. 58, 28–37.
Jhanwar-Uniyal, M., Gillick, J.L., Neil, J., Tobias, M., Thwing, Z.E., Murali, R., 2015. Distinct signaling mechanisms of mTORC1 and mTORC2 in glioblastoma multiforme: a tale of two complexes. Adv. Biol. Regul. 57, 64–74.
Jhanwar-Uniyal, M., Amin, A.G., Cooper, J.B., Das, K., Schmidt, M.H., Murali, R., 2017. Discrete signaling mechanisms of mTORC1 and mTORC2: connected yet apart in cellular and molecular aspects. Adv. Biol. Regul. 64, 39–48.
Jiang, J., Feng, X., Zhou, W., Wu, Y., Yang, Y., 2016. MiR-128 reverses the gefitinib resistance of the lung cancer stem cells by inhibiting the c-met/PI3K/AKT pathway. Oncotarget 7, 73188–73199.
Jin, H., Qiao, F., Wang, Y., Xu, Y., Shang, Y., 2015. Curcumin inhibits cell proliferation and induces apoptosis of human non-small cell lung cancer cells through the upregulation of miR-192-5p and suppression of PI3K/Akt signaling pathway. Oncol. Rep. 34, 2782–2789.
Kang, D.S., Yang, Y.R., Lee, C., Kim, S., Ryu, S.H., Suh, P.G., 2016. Roles of phosphoinositide-specific phospholipase Cγ1 in brain development. Adv. Biol. Regul. 60, 167–173.
Kato, A., Naiki-Ito, A., Nakazawa, T., Hayashi, K., Naitoh, I., Miyabe, K., Shimizu, S., Kondo, H., Nishi, Y., Yoshida, M., Umemura, S., Hori, Y., Mori, T., Tsutsumi, M., Kuno, T., Suzuki, S., Kato, H., Ohara, H., Joh, T., Takahashi, S., 2015. Chemopreventive effect of resveratrol and apocynin on pancreatic carcinogenesis via modulation of nuclear phosphorylated GSK3β and ERK1/2. Oncotarget 6, 42963–42975.
Kawaguchi, K., Igarashi, K., Murakami, T., Kiyuna, T., Lwin, T.M., Hwang, H.K., Delong, J.C., Clary, B.M., Bouvet, M., Unno, M., Hoffman, R.M., 2017. MEK inhibitors cobimetinib and trametinib, regressed a gemcitabine-resistant pancreatic-cancer patient-derived orthotopic xenograft (PDOX). Oncotarget 8, 47490–47496.
Kim, A., Seong, K.M., Kang, H.J., Park, S., Lee, S.S., 2015. Inhibition of Lyn is a promising treatment for mantle cell lymphoma with bortezomib resistance. Oncotarget 6, 38225–38238.
Kim, S.A., Kwon, Y., Kim, J.H., Muller, M.T., Chung, I.K., 1998. Induction of topoisomerase II mediated DNA cleavage by a protoberberine alkaloid, berberrubine. Biochemistry 37, 16316–16324.
Kizhakkayil, J., Thayyullathil, F., Chathoth, S., Hago, A., Patel, M., Galadari, S., 2010. Modulation of curcumin-induced Akt phosphorylation and apoptosis by PI3K inhibitor in MCF-7 cells. Biochem. Biophys. Res. Commun. 394, 476–481.
Kriplani, N., Hermida, M.A., Brown, E.R., Leslie, N.R., 2015. Class I PI 3-kinases: function and evolution. Adv. Biol. Regul. 59, 53–64.
Kumari, A., Parida, A.K., Rangani, J., Panda, A., 2017. Antioxidant activities, metabolic profiling, proximate analysis, mineral nutrient composition of Salvadora persica fruit unravel a potential functional food and a natural source of pharmaceuticals. Front. Pharmacol. 8, 61.
Leshchenko, V.V., Kuo, P.Y., Jiang, Z., Weniger, M.A., Overbey, J., Dunleavy, K., Wilson, W.H., Wiestner, A., Parekh, S., 2015. Harnessing Noxa demethylation to overcome Bortezomib resistance in mantle cell lymphoma. Oncotarget 6, 27332–27342.
Li, B., Ma, X., Kong, F., Zheng, C., Bjorkholm, M., Jia, J., Xu, D., 2015. Bortezomib-mediated down-regulation of telomerase and disruption of telomere homeostasis contributes to apoptosis of malignant cells. Oncotarget 6, 38079–38092.
Li, Q., Zhan, M., Chen, W., Zhao, B., Yang, K., Yang, J., Yi, J., Huang, Q., Mohan, M., Hou, Z., Wang, J., 2016. Phenylethyl isothiocyanate reverses cisplatin resistance in biliary tract cancer cells via glutathionylation-dependent degradation of Mcl-1. Oncotarget 7, 10271–10282.
Lim, S.M., Park, H.S., Kim, S., Kim, S., Ali, S.M., Greenbowe, J.R., Yang, I.S., Kwon, N.J., Lee, J.L., Ryu, M.H., Ahn, J.H., Lee, J., Lee, M.G., Kim, H.S., Kim, H., Kim, H.R., Moon, Y.W., Chung, H.C., Kim, J.H., Kang, Y.K., Cho, B.C., 2016. Next-generation sequencing reveals somatic mutations that confer exceptional response to everolimus. Oncotarget 7, 10547–10556.
Lin, C.J., Chen, T.H., Yang, L.Y., Shih, C.M., 2014. Resveratrol protects astrocytes against traumatic brain injury through inhibiting apoptotic and autophagic cell death. Cell Death Dis. 5, e1147.
Liu, B., Wang, G., Yang, J., Pan, X., Yang, Z., Zang, L., 2011. Berberine inhibits human hepatoma cell invasion without cytotoxicity in healthy hepatocytes. PLoS One 6, e21416.
Liu, M., Yang, X., Liu, J., Zhao, B., Ca, W., Li, Y., Hu, D., 2017. Efficacy and safety of BRAF inhibition alone versus combined BRAF and MEK inhibition in melanoma: a meta-analysis of randomized controlled trials. Oncotarget 8, 32258–32269.
Liu, Q., Yuan, W., Tong, D., Liu, G., Lan, W., Zhang, D., Xiao, H., Zhang, Y., Huang, Z., Yang, J., Zhang, J., Jiang, J., 2016. Metformin represses bladder cancer progression by inhibiting stem cell repopulation via COX2/PGE2/STAT3 axis. Oncotarget 7, 28235–28246.
Lupieri, A., Smirnova, N., Malet, N., Gayral, S., Laffargue, M., 2015. PI3K signaling in arterial diseases: non-redundant functions of the PI3K isoforms. Adv. Biol. Regul. 59, 4–18.
Maczis, M., Milstien, S., Spiegel, S., 2016. Sphingosine-1-phosphate and estrogen signaling in breast cancer. Adv. Biol. Regul. 60, 160–165.
McCarty, M.F., 2006. Isoflavones made simple - genistein's agonist activity for the beta-type estrogen receptor mediates their health benefits. Med. Hypotheses 66, 1093–1114.
McCubrey, J.A., Abrams, S.L., Umezawa, K., Cocco, L., Martelli, A.M., Franklin, R.A., Chappell, W.H., Steelman, L.S., 2012a. Novel approaches to target cancer initiating cells-eliminating the root of the cancer. Adv. Biol. Regul. 52, 249–264.
McCubrey, J.A., Steelman, L.S., Chappell, W.H., Abrams, S.L., Franklin, R.A., Montalto, G., Cervello, M., Libra, M., Candido, S., Malaponte, G., Mazzarino, M.C., Fagone, P., Nicoletti, F., Bäsecke, J., Mijatovic, S., Maksimovic-Ivanic, D., Milella, M., Tafuri, A., Chiarini, F., Evangelisti, C., Cocco, L., Martelli, A.M., 2012b. Ras/Raf/MEK/ERK and PI3K/PTEN/Akt/mTOR cascade inhibitors: how mutations can result in therapy resistance and how to overcome resistance. Oncotarget 3, 1068–1111.
McCubrey, J.A., Steelman, L.S., Chappell, W.H., Abrams, S.L., Montalto, G., Cervello, M., Nicoletti, F., Fagone, P., Malaponte, G., Mazzarino, M.C., Candido, S., Libra, M., Bäsecke, J., Mijatovic, S., Maksimovic-Ivanic, D., Milella, M., Tafuri, A., Cocco, L., Evangelisti, C., Chiarini, F., Martelli, A.M., 2012c. Mutations and deregulation of Ras/Raf/MEK/ERK and PI3K/PTEN/Akt/mTOR cascades which alter therapy response. Oncotarget 3, 954–987.
McCubrey, J.A., Steelman, L.S., Bertrand, F.E., Davis, N.M., Abrams, S.L., Montalto, G., D'Assoro, A.B., Libra, M., Nicoletti, F., Maestro, R., Basecke, J., Cocco, L., Cervello, M., Martelli, A.M., 2014a. Multifaceted roles of GSK-3 and Wnt/β-catenin in hematopoiesis and leukemogenesis: opportunities for therapeutic intervention. Leukemia 28, 15–33.
McCubrey, J.A., Steelman, L.S., Bertrand, F.E., Davis, N.M., Sokolosky, M., Abrams, S.L., Montalto, G., D'Assoro, A.B., Libra, M., Nicoletti, F., Maestro, R., Basecke, J., Rakus, D., Gizak, A., Demidenko, Z.N., Cocco, L., Martelli, A.M., Cervello, M., 2014b. GSK-3 as potential target for therapeutic intervention in cancer. Oncotarget 5, 2881–2911.
McCubrey, J.A., Davis, N.M., Abrams, S.L., Montalto, G., Cervello, M., Basecke, J., Libra, M., Nicoletti, F., Cocco, L., Martelli, A.M., Steelman, L.S., 2014c. Diverse roles of GSK-3: tumor promoter-tumor suppressor, target in cancer therapy. Adv. Biol. Regul. 54, 176–196.
McCubrey, J.A., Abrams, S.L., Fitzgerald, T.L., Cocco, L., Martelli, A.M., Montalto, G., Cervello, M., Scalisi, A., Candido, S., Libra, M., Steelman, L.S., 2015. Roles of signaling pathways in drug resistance, cancer initiating cells and cancer progression and metastasis. Adv. Biol. Regul. 57, 75–101.
McCubrey, J.A., Rakus, D., Gizak, A., Steelman, L.S., Abrams, S.L., Lertpiriyapong, K., Fitzgerald, T.L., Yang, L.V., Montalto, G., Cervello, M., Libra, M., Nicoletti, F., Scalisi, A., Torino, F., Fenga, C., Neri, L.M., Marmiroli, S., Cocco, L., Martelli, A.M., 2016. Effects of mutations in Wnt/β-catenin, hedgehog, Notch and PI3K pathways on GSK-3 activity- Diverse effects on cell growth, metabolism and cancer. Biochim. Biophys. Acta 1863, 2942–2976.
McCubrey, J.A., Lertpiriyapong, K., Steelman, L.S., Abrams, S.L., Yang, L.V., Murata, R.M., Rosalen, P.L., Scalisi, A., Neri, L.M., Cocco, L., Ratti, S., Martelli, A.M., Laidler, P., Dulińska-Litewka, J., Rakus, D., Gizak, A., Lombardi, P., Nicoletti, F., Candido, S., Libra, M., Montalto, G., Cervello, M., 2017a. Effects of resveratrol, curcumin, berberine and other nutraceuticals on aging, cancer development, cancer stem cells and microRNAs. Aging (Albany NY) 9, 1477–1536.
McCubrey, J.A., Lertpiriyapong, K., Steelman, L.S., Abrams, S.L., Cocco, L., Ratti, S., Martelli, A.M., Candido, S., Libra, M., Montalto, G., Cervello, M., Gizak, A., Rakus, D., 2017b. Regulation of GSK-3 activity by curcumin, berberine and resveratrol: potential effects on multiple diseases. Adv. Biol. Regul. 65, 77–88.
McCubrey, J.A., Fitzgerald, T.L., Yang, L.V., Lertpiriyapong, K., Steelman, L.S., Abrams, S.L., Montalto, G., Cervello, M., Neri, L.M., Cocco, L., Martelli, A.M., Laidler, P., Dulinska-Litewka, J., Rakus, D., Gizak, A., Nicoletti, F., Falzone, L., Candido, S., Libra, M., 2017c. Roles of GSK-3 and microRNAs on epithelial mesenchymal transition and cancer stem cells. Oncotarget 8, 14221–14250.
McCubrey, J.A., Cocco, L., 2017. GSK-3 signaling in health. Adv. Biol. Regul. 65, 1–4.
McCubrey, J.A., Lertpiriyapong, K., Fitzgerald, T.L., Martelli, A.M., Cocco, L., Rakus, D., Gizak, A., Libra, M., Cervello, M., Montalto, G., Yang, L.V., Abrams, S.L.,

Steelman, L.S., 2017d. Roles of TP53 in determining therapeutic sensitivity, growth, cellular senescence, invasion and metastasis. Adv. Biol. Regul. Adv. Biol. Regul. 63, 32–48.
Mérida, I., Torres-Ayuso, P., Ávila-Flores, A., Arranz-Nicolás, J., Andrada, E., Tello-Lafo, M., Liébana, R., Arcos, R., 2017. Diacylglycerol kinases in cancer. Adv. Biol. Regul. 63, 22–31.
Mikoshiba, K., 2015. Role of IP3 receptor signaling in cell functions and diseases. Adv. Biol. Regul. 57, 217–227.
Mitra, A., Mishra, L., Li, S., 2015. EMT, CTCs and CSCs in tumor relapse and drug-resistance. Oncotarget 6, 10697–10711.
Mollinedo, F., Gajate, C., 2015. Lipid rafts as major platforms for signaling regulation in cancer. Adv. Biol. Regul. 57, 130–146.
Montesano, A., Luzi, L., Senesi, P., Mazzocchi, N., Terruzzi, I., 2013. Resveratrol promotes myogenesis and hypertrophy in murine myoblasts. J. Transl. Med. 11, 310.
Montraveta, A., Xargay-Torrent, S., Rosich, L., Lopez-Guerra, M., Roldan, J., Rodriguez, V., Lee-Verges, E., de Frias, M., Campas, C., Campo, E., Roue, G., Colomer, D., 2015. Bcl-2high mantle cell lymphoma cells are sensitized to acadesine with ABT-199. Oncotarget 6, 21159–21172.
Nelson, K.M., Dahlin, J.L., Bisson, J., Graham, J., Pauli, G.F., Walters, M.A., 2017. The essential medicinal chemistry of curcumin. J. Med. Chem. 60, 1620–1637.
Nishida, T., Hattori, K., Watanabe, K., 2017. The regulatory and signaling mechanisms of the ASK family. Adv. Biol. Regul. 30119–30127 Pii: S2212–4926.
Nunes-Xavier, C.E., Elson, A., Pulido, R., 2012. Epidermal growth factor receptor (EGFR)-mediated positive feedback of protein-tyrosine phosphatase epsilon (PTPepsilon) on ERK1/2 and AKT protein pathways is required for survival of human breast cancer cells. J. Biol. Chem. 287, 3433–3444.
Olayanju, B., Hampsey, J.J., Hampsey, M., 2015. Genetic analysis of the Warburg effect in yeast. Adv. Biol. Regul. 57, 185–192.
Pappas, L., Xu, X.L., Abramson, D.H., Jawar, S.C., 2017. Genomic instability and proliferation/survival pathways in RB1-deficient malignancies. Adv. Biol. Regul. 64, 20–32.
Park, S.Y., Kim, M.J., Park, S.A., Kim, J.S., Min, K.N., Kim, D.K., Lim, W., Nam, J.S., Sheen, Y.Y., 2015. Combinatorial TGF-beta attenuation with paclitaxel inhibits the epithelial-to- transition and breast cancer stem-like cells. Oncotarget 6, 37526–37543.
Patel, M., Gupta, A., Dey, C.S., 2011. Potentiation of neuronal insulin signaling and glucose uptake by resveratrol: the involvement of AMPK. Pharmacol. Rep. 63, 1162–1168.
Perdios, L., Bunney, T.D., Warren, S.C., Dunsby, C., French, P.M., Tate, E.W., Katan, M., 2016. Time-resolved FRET reports FGFR1 dimerization and formation of a complex with its effector PLCγ1. Adv. Biol. Regul. 60, 6–13.
Ponnurangam, S., Dandawate, P.R., Dhar, A., Tawfik, O.W., Parab, R.R., Mishra, P.D., Ranadive, P., Sharma, R., Mahajan, G., Umar, S., Weir, S.J., Sugumar, A., Jensen, R.A., Padhye, S.B., Balakrishnan, A., Anant, S., Subramaniam, D., 2016. Quinomycin A targets Notch signaling pathway in pancreatic cancer stem cells. Oncotarget 7, 3217–3232.
Prasad, A., Khudaynazar, N., Tantravahi, R.V., Gillum, A.M., Hoffman, B.S., 2016. ON 01910.Na (rigosertib) inhibits PI3K/Akt pathway and activates oxidative stress signals in head and neck cancer cell lines. Oncotarget 7, 79388–79400.
Prasad, S., Gupta, S.C., Tyagi, A.K., 2017. Reactive oxygen species (ROS) and cancer: role of antioxidative nutraceuticals. [Review]. Cancer Lett. 387, 95–105.
Pyne, N.J., McNaughton, M., Boomkamp, S., MacRitchie, N., Evangelisti, C., Martelli, A.M., Jiang, H.R., Ubhi, S., Pyne, S., 2016. Role of sphingosine 1-phosphate receptors, sphingosine kinases and sphingosine in cancer and inflammation. Adv. Biol. Regul. 60, 151–159.
Qian, X.J., Li, Y.T., Yu, Y., Yang, F., Deng, R., Ji, J., Jiao, L., Li, X., Wu, R.Y., Chen, W.D., Feng, G.K., Zhu, X.F., 2015. Inhibition of DNA methyltransferase as a novel therapeutic strategy to overcome acquired resistance to dual PI3K/mTOR inhibitors. Oncotarget 6, 5134–5146.
Qin, Y., Pang, J.Y., Chen, W.H., Zhao, Z.Z., Liu, L., Jiang, Z.H., 2007. Inhibition of DNA topoisomerase I by natural and synthetic mono- and dimeric protoberberine alkaloids. Chem. Biodivers. 4, 481–487.
Raben, D.M., Barber, C.N., 2017. Phosphatidic acid and neurotransmission. Adv. Biol. Regul. 63, 15–21.
Ramazzotti, G., Faenza, I., Fiume, R., Billi, A.M., Manzoli, L., Mongiorgi, S., Ratti, S., McCubrey, J.A., Suh, P.G., Cocco, L., Follo, M.Y., 2017. PLC-β1 and cell differentiation: an insight into myogenesis and osteogenesis. Adv. Biol. Regul. 63, 1–5.
Reddyvari, H., Govatati, S., Matha, S.K., Korla, S.V., Malempati, S., Pasupuleti, S.R., Bhanoori, M., Nallanchakravarthula, V., 2017. Therapeutic effect of green tea extract on alcohol induced hepatic mitochondrial DNA damage in albino wistar rats. J. Adv. Res. 8, 289–295.
Ren, H., Guo, H., Thakur, A., Zhang, S., Wang, T., Liang, Y., Shi, P., Gao, L., Liu, F., Feng, J., Chen, T., Yang, T., Shang, D., Liu, J.J., Xu, F., Chen, M., 2016. Blockade efficacy of MEK/ERK-dependent autophagy enhances PI3K/Akt inhibitor NVP-BKM120's therapeutic effectiveness in lung cancer cells. Oncotarget 7, 67277–67287.
Ricciardi, M.R., Mirabilii, S., Licchetta, R., Piedimonte, M., Tafuri, A., 2017. Targeting the Akt, GSK-3, Bcl-2 axis in acute myeloid leukemia. Adv. Biol. Regul. 65, 36–58.
Rinkenbaugh, A.L., Cogswell, P.C., Calamini, B., Dunn, D.E., Persson, A.I., Weiss, W.A., Lo, D.C., Baldwin, A.S., 2016. IKK/NF-kappaB signaling contributes to glioblastoma stem cell maintenance. Oncotarget 7, 69173–69187.
Rohacs, T., 2016. Phosphoinositide signaling in somatosensory neurons. Adv. Biol. Regul. 61, 2–16.
Rommel, C., Bodine, S.C., Clarke, B.A., Rossman, R., Nunez, L., Stitt, T.N., Yancopoulos, G.D., Glass, D.J., 2001. Mediation of IGF-1-induced skeletal myotube hypertrophy by PI(3)K/Akt/mTOR and PI(3)K/Akt/GSK3 pathways. Nat. Cell Biol. 3, 1009–1013.
Rumman, M., Jung, K.H., Fang, Z., Yan, H.H., Son, M.K., Kim, S.J., Kim, J., Park, J.H., Lim, J.H., Hong, S., Hong, S.S., 2016. HS-173, a novel PI3K inhibitor suppresses EMT and metastasis in pancreatic cancer. Oncotarget 7, 78029–78047.
Russo, M.A., Sansone, L., Polletta, L., Runci, A., Rashid, M.M., De Santis, E., Vernucci, E., Carnevale, I., Tafani, M., 2014. Sirtuins and resveratrol-derived compounds: a model for understanding the beneficial effects of the Mediterranean diet. Endocr. Metab. Immune Disord. Drug Targets 14, 300–308.
Ruvolo, P.P., 2017. GSK-3 as a novel prognostic indicator in leukemia. Adv. Biol. Regul. 65, 26–35.
Ruzzene, M., Bertacchini, J., Toker, A., Marmiroli, S., 2017. Cross-talk between the CK2 and AKT signaling pathways in cancer. Adv. Biol. Regul. 64, 1–8.
Ryuno, H., Naguro, I., Kamiyama, M., 2017. ASK family and cancer. Adv. Biol. Regul. 30114–30118 pii: S2212–4926.
Scarlata, S., Garwain, O., Williams, L., Burguera, I.G., Rosati, B., Sahu, S., Guo, Y., Philip, F., Golebiewska, U., 2016. Phospholipase Cβ connects G protein signaling with RNA interference. Adv. Biol. Regul. 61, 51–57.
Schnerch, D., Schuler, J., Follo, M., Felthaus, J., Wider, D., Klingner, K., Greil, C., Duyster, J., Engelhardt, M., Wasch, R., 2017. Proteasome inhibition enhances the efficacy of volasertib-induced mitotic arrest in AML in vitro and prolongs survival in vivo. Oncotarget 8, 21153–21166.
Schrock, M.S., Karras, J.R., Guggenbiller, M.J., Druck, T., Batar, B., Huebner, K., 2017. Fhit and Wwox loss-associated genome instability: a genome caretaker one-two punch. Adv. Biol. Regul. 63, 167–176.
Schurmans, S., Polizzi, S., Scoumanne, A., Sayyed, S., Molina-Ortiz, P., 2015. The Ras/Rap GTPase activating protein RASA3: from gene structure to in vivo functions. Adv. Biol. Regul. 57, 153–161.
Scoumanne, A., Molina-Ortiz, P., Monteyne, D., Perez-Morga, D., Erneux, C., Schurmans, S., 2016. Specific expression and function of inositol 1,4,5-trisphosphate 3-kinase C (ITPKC) in wild type and knock-out mice. Adv. Biol. Regul. 62, 1–10.
Seo, E.J., Kim, D.K., Jang, I.H., Choi, E.J., Shin, S.H., Lee, S.I., Kwon, S.M., Kim, K.H., Suh, D.S., Kim, J.H., 2016. Hypoxia-NOTCH1-SOX2 signaling is important for maintaining cancer stem cells in ovarian cancer. Oncotarget 7, 55624–55638.
Shamseddine, A.A., Airola, M.V., Hannun, Y.A., 2015. Roles and regulation of neutral sphingomyelinase-2 in cellular and pathological processes. Adv. Biol. Regul. 57, 24–41.
Shears, S.B., 2015. Inositol pyrophosphates: why so many phosphates? Adv. Biol. Regul. 57, 203–216.
Shears, S.B., Baughman, B.M., Gu, C., Nair, V.S., Wang, H., 2017. The significance of the 1-kinase/1-phosphatase activities of the PPIP5K family. Adv. Biol. Regul. 63, 98–106.
Shin, S.M., Cho, I.J., Kim, S.G., 2009. Resveratrol protects mitochondria against oxidative stress through AMP-activated protein kinase-mediated glycogen synthase kinase-3beta inhibition downstream of poly(ADP-ribose) polymerase-LKB1 pathway. Mol. Pharmacol. 76, 884–895.
Sibbesen, N.A., Kopp, K.L., Litvinov, I.V., Jønson, L., Willerslev-Olsen, A., Fredholm, S., Petersen, D.L., Nastasi, C., Krejsgaard, T., Lindahl, L.M., Gniadecki, R., Mongan, N.P., Sasseville, D., Wasik, M.A., Iversen, L., Bonefeld, C.M., Geisler, C., Woetmann, A., Odum, N., 2015. Jak3, STAT3, and STAT5 inhibit expression of miR-22, a novel tumor suppressor microRNA, in cutaneous T-Cell lymphoma. Oncotarget 6, 20555–20569.
Simão, F., Matté, A., Pagnussat, A.S., Netto, C.A., Salbego, C.G., 2012. Resveratrol prevents CA1 neurons against ischemic injury by parallel modulation of both GSK-3â

and CREB through PI3-K/Akt pathways. Eur. J. Neurosci. 36, 2899–2905.
Singha, B., Gatla, H.R., Phyo, S., Patel, A., Chen, Z.S., Vancurova, I., 2015. IKK inhibition increases bortezomib effectiveness in ovarian cancer. Oncotarget 6, 26347–26358.
Spinelli, L., Lindsay, Y.E., Leslie, N.R., 2015. PTEN inhibitors: an evaluation of current compounds. Adv. Biol. Regul. 57, 102–111.
Su, Y.J., Lin, W.H., Chang, Y.W., Wei, K.C., Liang, C.L., Chen, S.C., Lee, J.L., 2015. Polarized cell migration induces cancer type-specific CD133/integrin/Src/Akt/GSK3beta/beta-catenin signaling required for maintenance of cancer stem cell properties. Oncotarget 6, 38029–38045.
Tanaka, T., Tsuchiya, R., Hozumi, Y., Nakano, T., Okada, M., Goto, K., 2016. Reciprocal regulation of p53 and NF-κB by diacylglycerol kinase ζ. Adv. Biol. Regul. 60, 15–21.
Tao, Y.F., Pang, L., Du, X.J., Sun, L.C., Hu, S.Y., Lu, J., Cao, L., Zhao, W.L., Feng, X., Wang, J., Wu, D., Wang, N., Ni, J., Pan, J., 2013. Differential mRNA expression levels of human histone-modifying enzymes in normal karyotype B cell pediatric acute lymphoblastic leukemia. Int. J. Mol. Sci. 14, 3376–3394.
Thounaojam, M.C., Dudimah, D.F., Pellom Jr., S.T., Uzhachenko, R.V., Carbone, D.P., Dikov, M.M., Shanker, A., 2015. Bortezomib enhances expression of effector molecules in anti-tumor CD8+ T lymphocytes by promoting Notch-nuclear factor-kappaB crosstalk. Oncotarget 6, 32439–32455.
Tillhon, M., Guamán Ortiz, L.M., Lombardi, P., Scovassi, A.I., 2012. Berberine: new perspectives for old remedies. Biochem. Pharmacol. 84, 1260–1267.
Tomita, T., 2017. Aberrant proteolytic processing and therapeutic strategies in Alzheimer disease. Adv. Biol. Regul. 64, 33–38.
Tsai, J.H., Hsu, L.S., Lin, C.L., Hong, H.M., Pan, M.H., Way, T.D., Chen, W.J., 2013. 3,5,4'-Trimethoxystilbene, a natural methoxylated analog of resveratrol, inhibits breast cancer cell invasiveness by downregulation of PI3K/Akt and Wnt/β-catenin signaling cascades and reversal of epithelial-mesenchymal transition. Toxicol. Appl. Pharmacol. 272, 746–756.
Tzeng, H.E., Yang, L., Chen, K., Wang, Y., Liu, Y.R., Pan, S.L., Gaur, S., Hu, S., Yen, Y., 2015. The pan-PI3K inhibitor GDC-0941 activates canonical WNT signaling to confer resistance in TNBC cells: resistance reversal with WNT inhibitor. Oncotarget 6, 11061–11073.
Tu-Sekine, B., Goldschmidt, H., Raben, D.M., 2015. Diacylglycerol, phosphatidic acid, and their metabolic enzymes in synaptic vesicle recycling. Adv. Biol. Regul. 57, 147–152.
Varamini, B., Sikalidis, A.K., Bradford, K.L., 2014. Resveratrol increases cerebral glycogen synthase kinase phosphorylation as well as protein levels of drebrin and transthyretin in mice: an exploratory study. Int. J. Food Sci. Nutr. 65, 89–96.
Vergara, D., Simeone, P., Toraldo, D., Del Boccio, P., Vergaro, V., Leporatti, S., Pieragostino, D., Tinelli, A., De Domenico, S., Alberti, S., Urbani, A., Salzet, M., Santino, A., Maffia, M., 2012. Resveratrol downregulates Akt/GSK and ERK signalling pathways in OVCAR-3 ovarian cancer cells. Mol. Biosyst. 8, 1078–1087.
Wang, N., Feng, Y., Zhu, M., Tsang, C.M., Man, K., Tong, Y., Tsao, S.W., 2010a. Berberine induces autophagic cell death and mitochondrial apoptosis in liver cancer cells: the cellular mechanism. J. Cell Biochem. 111, 1426–1436.
Wang, H., Zhou, H., Zou, Y., Liu, Q., Guo, C., Gao, G., Shao, C., Gong, Y., 2010b. Resveratrol modulates angiogenesis through the GSK3β/β-catenin/TCF-dependent pathway in human endothelial cells. Biochem. Pharmacol. 80, 1386–1395.
Wang, S.Q., Wang, C., Chang, L.M., Zhou, K.R., Wang, J.W., Ke, Y., Yang, D.X., Shi, H.G., Wang, R., Shi, X.L., Ma, L.Y., Liu, H.M., 2016. Geridonin and paclitaxel act synergistically to inhibit the proliferation of gastric cancer cells through ROS-mediated regulation of the PTEN/PI3K/Akt pathway. Oncotarget 7, 72990–73002.
Wang, Y., Kheir, M.M., Chai, Y., Hu, J., Xing, D., Lei, F., Du, L., 2011. Comprehensive study in the inhibitory effect of berberine on gene transcription, including TATA box. PLoS ONE 6, e23495.
Wang, Y., Liu, Q., Liu, Z., Li, B., Sun, Z., Zhou, H., Zhang, X., Gong, Y., Shao, C., 2012. Berberine, a genotoxic alkaloid, induces ATM-Chk1 mediated G2 arrest in prostate cancer cells. Mutat. Res. 734, 20–29.
Wang, Z., Wang, N., Liu, P., Peng, F., Tang, H., Chen, Q., Xu, R., Dai, Y., Lin, Y., Xie, X., Peng, C., Situ, H., 2015. Caveolin-1, a stress-related oncotarget, in drug resistance. [Review]. Oncotarget 6, 37135–37150.
Weyhenmeyer, B.C., Noonan, J., Wurstle, M.L., Lincoln, F.A., Johnston, G., Rehm, M., Murphy, B.M., 2016. Predicting the cell death responsiveness and sensitization of glioma cells to TRAIL and temozolomide. Oncotarget 7, 61295–61311.
Xi, J., Wang, H., Mueller, R.A., Norfleet, E.A., Xu, Z., 2009. Mechanism for resveratrol-induced cardioprotection against reperfusion injury involves glycogen synthase kinase 3beta and mitochondrial permeability transition pore. Eur. J. Pharmacol. 604, 111–116.
Xiao, N., Chen, S., Ma, Y., Qiu, J., Tan, J.H., Ou, T.M., Gu, L.Q., Huang, Z.S., Li, D., 2012. Interaction of berberine derivative with protein POT1 affect telomere function in cancer cells. Biochem. Biophysical Res. Commun. 419, 567–572.
Xu, S., Fu, G.B., Tao, Z., OuYang, J., Kong, F., Jiang, B.H., Wan, X., Chen, K., 2015. MiR-497 decreases cisplatin resistance in ovarian cancer cells by targeting mTOR/P70S6K1. Oncotarget 6, 26457–26471.
Yamauchi, Y., Miura, Y., Kanaho, Y., 2017. Machineries regulating the activity of the small GTPase Arf6 in cancer cells are potential targets for developing innovative anti-cancer drugs. Adv. Biol. Regul. 63, 115–121.
Yang, L., Zhang, S., George, S.K., Teng, R., You, X., Xu, M., Liu, H., Sun, X., Amin, H.M., Shi, W., 2015a. Targeting Notch1 and proteasome as an effective strategy to suppress T-cell lymphoproliferative neoplasms. Oncotarget 6, 14953–14969.
Yang, Z., Guo, L., Liu, D., Sun, L., Chen, H., Deng, Q., Liu, Y., Yu, M., Ma, Y., Guo, N., Shi, M., 2015b. Acquisition of resistance to trastuzumab in gastric cancer cells is associated with activation of IL-6/STAT3/Jagged-1/Notch positive feedback loop. Oncotarget 6, 5072–5087.
Yang, Y.R., Kang, D.S., Lee, C., Seok, H., Follo, M.Y., Cocco, L., Suh, P.G., 2016. Primary phospholipase C and brain disorders. Adv. Biol. Regul. 61, 80–85.
Yao, G., Zhang, Q., Doeppner, T.R., Niu, F., Li, Q., Yang, Y., Kuckelkorn, U., Hagemann, N., Li, W., Hermann, D.M., Dai, Y., Zhou, W., Jin, F., 2015. LDL suppresses angiogenesis through disruption of the HIF pathway via NF-kappaB inhibition which is reversed by the proteasome inhibitor BSc2118. Oncotarget 6, 30251–30262.
Ye, M., Zhang, J., Zhang, J., Miao, Q.L., Zhang, J., 2015. Curcumin promotes apoptosis by activating the p53-miR-192-5p/215-XIAP pathway in non-small cell lung cancer. Cancer Lett. 357, 196–205.
Yeh, Y.Y., Chen, R., Hessler, J., Mahoney, E., Lehman, A.M., Heerema, N.A., Grever, M.R., Plunkett, W., Byrd, J.C., Johnson, A.J., 2015. Up-regulation of CDK9 kinase activity and Mcl-1 stability contributes to the acquired resistance to cyclin-dependent kinase inhibitors in leukemia. Oncotarget 6, 2667–2679.
Yu, L., Fan, Z., Fang, S., Yang, J., Gao, T., Simoes, B.M., Eyre, R., Guo, W., Clarke, R.B., 2016. Cisplatin selects for stem-like cells in osteosarcoma by activating Notch signaling. Oncotarget 7, 33055–33068.
Yu, Z., Zhao, G., Xie, G., Zhao, L., Chen, Y., Yu, H., Zhang, Z., Li, C., Li, Y., 2015. Metformin and temozolomide act synergistically to inhibit growth of glioma cells and glioma stem cells in vitro and in vivo. Oncotarget 6, 32930–32943.
Zhang, R., Qiao, H., Chen, S., Chen, X., Dou, K., Wei, L., Zhang, J., 2016a. Berberine reverses lapatinib resistance of HER2-positive breast cancer cells by increasing the level of ROS. Cancer Biol. Ther. 17, 925–934.
Zhang, B., Zhao, R., He, Y., Fu, X., Fu, L., Zhu, Z., Fu, L., Dong, J.T., 2016b. MicroRNA 100 sensitizes luminal A breast cancer cells to paclitaxel treatment in part by targeting mTOR. Oncotarget 7, 5702–5714.
Zhang, Y., Liu, L., Fan, P., Bauer, N., Gladkich, J., Ryschich, E., Bazhin, A.V., Giese, N.A., Strobel, O., Hackert, T., Hinz, U., Gross, W., Fortunato, F., Herr, I., 2015. Aspirin counteracts cancer stem cell features, desmoplasia and gemcitabine resistance in pancreatic cancer. Oncotarget 6, 9999–10015.
Zhao, H., Halicka, H.D., Li, J., Darzynkiewicz, Z., 2013. Berberine suppresses gero-conversion from cell cycle arrest to senescence. Aging (Albany NY) 5, 623–636.
Zhong, Y., Li, X., Yu, D., Li, X., Li, Y., Long, Y., Yuan, Y., Ji, Z., Zhang, M., Wen, J.G., Nesland, J.M., Suo, Z., 2015. Application of mitochondrial pyruvate carrier blocker UK5099 creates metabolic reprogram and greater stem-like properties in LnCap prostate cancer cells in vitro. Oncotarget 6, 37758–37769.
Zhou, Q., Ye, M., Lu, Y., Zhang, H., Chen, Q., Huang, S., Su, S., 2015a. Curcumin Improves the Tumoricidal effect of mitomycin C by Suppressing ABCG2 expression in stem cell-like breast cancer cells. PLoS One 10, e0136694.
Zhou, W., Xu, J., Gelston, E., Wu, X., Zou, Z., Wang, B., Zeng, Y., Wang, H., Liu, A., Xu, L., Liu, Q., 2015b. Inhibition of Bcl-xL overcomes polyploidy resistance and leads to apoptotic cell death in acute myeloid leukemia cells. Oncotarget 6, 21557–21571.
Zucha, M.A., Wu, A.T., Lee, W.H., Wang, L.S., Lin, W.W., Yuan, C.C., Yeh, C.T., 2015. Bruton's tyrosine kinase (Btk) inhibitor ibrutinib suppresses stem-like traits in ovarian cancer. Oncotarget 6, 13255–13268.